Production of dissolved organic carbon by Arctic plankton communities: responses to elevated carbon dioxide and the availability of light and nutrients

Alex J. Poulton[a,*], Chris J. Daniels[a,b], Mario Esposito[a,b], Matthew P. Humphreys[b], Elaine Mitchell[c], Mariana Ribas-Ribas[b,d], Benjamin C. Russell[b], Mark C. Stinchcombe[a], Eithne Tynan[b] , Sophie Richier[b]

[a] Ocean Biogeochemistry and Ecosystems, National Oceanography Centre, Waterfront Campus, Southampton, UK.

[b] Ocean and Earth Sciences, University of Southampton, National Oceanography Centre Southampton, Southampton, UK.

[c] Scottish Association of Marine Sciences, Scottish Marine Institute, Oban, Argyll, UK.

[d] Carl von Ossietzky Universität Oldenburg, Institute for Chemistry and Biology of the Marine Environment, Wilhelmshaven, 26382, Germany.

* Corresponding Author. Tel: +44 2380 597086.

E-mail address: Alex.Poulton@noc.ac.uk (Alex Poulton).

Abstract

The extracellular release of dissolved organic carbon (DOC) by phytoplankton is a potentially important source of labile organic carbon for bacterioplankton in pelagic ecosystems. In the context of increasing seawater partial pressure of CO_2 (pCO_2), via the oceanic absorption of elevated atmospheric CO_2 (ocean acidification), several previous studies have reported increases to the relative amount of carbon fixed into particulates, via primary production (PP), and dissolved phases (DOC). During the summer of 2012 we measured DOC production by phytoplankton communities in the Nordic seas of the Arctic Ocean (Greenland, Norwegian and Barents Sea) from both *in situ* sampling and during three bioassay experiments where pCO_2 levels (targets ~550 μatm, ~750 μatm, ~1000 μatm) were elevated relative to ambient conditions. Measurements of DOC production and PP came from 24 h incubations and therefore represent net DOC production rates, where an unknown portion of the DOC released has potentially been utilized by heterotrophic organisms. Production of DOC (net *p*DOC) by *in situ* communities varied from 0.09 to 0.64 mmol C m^{-3} d^{-1} (average 0.25 mmol C m^{-3} d^{-1}), with comparative rates in two of the experimental bioassays (0.04 to 1.23 mmol C m^{-3} d^{-1}) and increasing dramatically in the third (up to 5.88 mmol C m^{-3} d^{-1}). When expressed as a fraction of total carbon fixation (i.e., PP plus *p*DOC), percentage extracellular release (PER) was 14% on average (range 2% to 46%) for *in situ* measurements, with PER in the three bioassays having a very similar range (2% to 50 %). A marked increase in *p*DOC (and PER) was only observed in one of the bioassays where nutrient levels (nitrate, silicic acid) dropped dramatically relative to starting (ambient) concentrations; no pCO_2 treatment effect on *p*DOC (or PER) was evident across the three experiments. Examination of *in situ* net *p*DOC (and PER) found significant correlations with decreasing silicic acid and increasing euphotic zone depth, indicating that nutrient and light availability were strong drivers of the partitioning of primary production between particulate and dissolved phases. Furthermore, the third bioassay experiment had relatively high levels of diatom biomass as well as a strong response to nitrate and silicic acid depletion, and we suggest that nutrient starved or light limited diatom communities may be strong producers of DOC in Arctic ecosystems.

Keywords:
Dissolved Organic Carbon; Arctic Ocean; Ocean Acidification; Phytoplankton; Bacteria; Diatoms.

1. Introduction

The production of dissolved organic carbon (*p*DOC) relates to the fraction of photosynthetically fixed carbon that is subsequently released to the extracellular medium in a dissolved form and can represent a substantial fraction (up to 50%) of gross primary production (i.e. the sum of particulate and dissolved carbon fixation) (Marañón et al., 2005; Hansell, 2002; Hansell and Carlson, 2015). Production of DOC is an important source of organic carbon to sustain heterotrophic bacterial growth and respiration (Cole et al., 1982; Hansell, 2002; Hansell and Carlson, 2015). Phytoplankton production of DOC can occur through passive diffusion of low molecular compounds through the cell membrane, especially from small cells due to their low surface area to volume ratio, and through active release under conditions of high light and nutrient stress (Kiørbe 1993; López-Sandoval et al., 2011). Microzooplankton sloppy feeding, excretion and egestion may also be important sources of DOC (Nagata, 2000; Marañón et al., 2005; Robinson, 2008), especially in low nutrient conditions which are dominated by small cells and where the percentage of extracellular release (PER = 100 x (*p*DOC / PP + *p*DOC)) may represent 20 to 40% of gross primary production (e.g., Karl et al., 1998; Teira et al., 2001, 2003; López-Sandoval et al., 2011).

Elevated *p*DOC (and PER) from cellular exudation under sub-optimal conditions for phytoplankton has been suggested to be a cellular mechanism to compensate for the uncoupling between high energy (light) and low nutrients (Marañón et al., 2005; López-Sandoval et al., 2011). However, *p*DOC can also result from a number of processes which are more related to community trophic interactions, such as sloppy feeding or viral lysis (Nagata, 2000), and hence it is important to consider how *p*DOC is measured when examining the source of DOC (Teira et al., 2001). A common method for measuring *p*DOC is through the separation of particulate and dissolved carbon fixation, with dissolved production representing *p*DOC. Radiolabelling (carbon-14) or using stable isotopes (carbon-13) potentially represents more accurate determinations of *p*DOC than time-series measurements of bulk DOC. Rapid utilization of photosynthetically fixed carbon by heterotrophic bacteria can also mask short-term DOC dynamics (Cole et al., 1982; Engel et al., 2004, 2013) making the source and trophic interactions of DOC producers and consumers complex to interpret. Due to this rapid utilization of released DOC, long incubations (12-24 h) measuring DOC production are likely to represent net DOC production, after a portion of the DOC has been respired by bacterioplankton, rather than gross DOC production.

Increased *p*DOC has also been linked to elevated pCO_2, where increased carbon availability leads to an increased proportion of gross primary production (PP) being released into the dissolved phase (Engel et al., 2013). Such elevated *p*DOC has been seen in several studies (e.g., Engel et al., 2013) using mesocosm and other experimental setups to manipulate the pCO_2 and pH

conditions of natural communities over timescales of days to weeks. However, such bioassays are often nutrient enriched during the experimental set up leading to increased DOC production during nutrient replete growth phases of the experiments (Czerny et al., 2013), although rapid utilization of freshly produced DOC by microbial elements of the community may again hide biogeochemical responses and relationships (Cole et al., 1982; Engel et al., 2004, 2013). Other studies have seen little or no response in *p*DOC (or PER) in experimentally manipulated communities, which may be linked to differing community structures, trophic interactions and environmental conditions (Yoshimura et al., 2010, 2013; Engel et al., 2004; Maugendre et al., 2015).

Examining the response of pelagic ecosystems to increased pCO_2 is a pressing concern in biological oceanography due to the phenomenon of Ocean Acidification (OA). The anthropogenic release of CO_2 into the atmosphere through fossil fuel burning has led to OA, whereby atmospheric CO_2 penetrates into the ocean declining surface ocean pH and perturbing the carbonate system from pre-industrial conditions (Royal Society, 2005; Fabry et al., 2009; Tynan et al., this issue). The solubility of CO_2 increases with decreasing water temperatures and hence polar waters in both hemispheres are expected to be amongst the first areas to experience dramatic changes in surface water pH (Royal Society, 2005; Fabry et al., 2009). The sensitivity of polar marine organisms and ecosystems to declining pH is currently unclear (Fabry et al., 2009), though several studies have focused on OA effects on pelagic biogeochemistry and food webs (e.g., the KOSMOS mesocosms in Kongsfjord, Svalbard, see Czerny et al., 2013; bioassays in the Bering Sea and subarctic Pacific, see Yoshimura et al., 2010, 2013).

As well as being susceptible to imminent changes in surface water carbon chemistry and pH, the Arctic Ocean is also experiencing increased temperatures which are causing earlier and more severe melting of seasonal ice in many regions (Boé et al., 2009; Fabry et al., 2009). The Arctic basin is subjected to significant riverine runoff which supplies large amounts of DOC to the Arctic Ocean (>200 mmol C m^{-3}), while inflowing water from the Atlantic and Pacific Oceans have concentrations ~50 mmol C m^{-3} (Anderson, 2002). Whilst some of this DOC is refractory and not directly available for biological uptake, high PP over the continental shelves and in association with ice edge blooms are also potentially significant sources of labile DOC through the release from algal cells or via sloppy feeding by zooplankton or viral lysis (Nagata, 2000). Recent measurements of bacterial respiration have shown that they represent a large fraction of total community respiration, indicating that bacteria play a key role in Arctic biogeochemistry and the marine carbon cycle in high latitude waters (Garcia-Martin et al., 2014a, 2014b). In an increasingly ice-free Arctic Ocean, the supply and biological sinks for DOC are likely to undergo rapid changes and hence understanding DOC dynamics is important to studies concerned with marine ecosystems under future climate forcing.

The high susceptibility of Arctic Ocean marine ecosystems and biogeochemistry to OA and strong changes in seasonal ice melt magnitude and timing (Boé et al., 2009; Fabry et al., 2009) made the Arctic Ocean a natural focus for the UK OA programme (Tynan et al., this issue). In this context, the present study examines the production of dissolved organic carbon (*p*DOC) in Arctic communities sampled during the summer of 2012 (Fig. 1), both in natural *in situ* settings and within a number (n = 3) of experimental bioassays (with methodology identical to Richier et al., 2014) designed to examine the sensitivity of Arctic plankton to variability in pH and pCO_2. It should be noted that due to the 24 h incubations of samples to determine PP and *p*DOC, these represent net rather than gross values (i.e. they do include respiratory losses). The overall aim of this study was two-fold: firstly to examine *p*DOC by unperturbed plankton communities; and secondly to examine *p*DOC in plankton communities exposed to elevated pCO_2 (550-1000 μatm). In both instances, *p*DOC is also examined in the context of environmental conditions and plankton community structure.

2. Methodology

2.1. Water sampling

Water samples were collected during June 2012 from 19 stations in the Atlantic sector of the Arctic Ocean (Fig. 1a) during cruise 271 of the RRS *James Clark Ross* (JR271). Stations sampled included (Table 1): the Iceland-Faroes Front (C019); several stations in the Greenland Sea (C020, C021, C060, C063); several stations near the Greenland Ice Shelf, either in the ice-edge (C029, C040) or in the ice (C027, C030, C032, C033); Fram Strait (C042); several stations in the Barents Sea (C047, C052, C054); several stations in the Norwegian Sea (C045, C056, C058); and one to the north of Iceland (C065). The Greenland Sea had sea surface temperatures <5 ^{o}C, while the Norwegian Sea stations had sea surface temperatures >5 ^{o}C (Table 1, Fig. 1b). Stations in the Barents Sea were identified as being above the continental shelf (Fig. 1a), although clearly C047 was cold-water influenced due to the low SST in the northern Barents Sea (Fig. 1b, Table 1).

Water samples were collected from the middle of the mixed layer (10-30 m) in 20 L Niskin bottles on a CTD rosette sampler. Water samples from Niskin bottles were drawn into sample bottles for measurements of primary production (PP), total and >10 μm chlorophyll-*a* (Chl), bacterial production (BP), bacterial biomass (C_{bact}), macronutrient (nitrate, NOx; phosphate, PO_4; silicic acid, dSi) concentrations, carbonate chemistry parameters (dissolved inorganic carbon, total alkalinity) and particulate silica ($bSiO_2$).

Sea-surface temperatures and salinities were taken from the CTD, with mixed layer depths estimated from the vertical density profiles. Daily incidental irradiance ($Ed_{[0+]}$), for Photosynthetically Active Radiation (PAR), was integrated from dawn to dusk (mol photons m^{-2} d^{-1}) from the RRS James Clark Ross 2 π PAR irradiance sensor (Skye Instruments, SKE 510). The vertical diffuse attenuation coefficient of PAR (K_d) in the water-column was calculated from early morning CTD stations, with the depth of the euphotic zone (Z_{eup}) calculated as the depth where 1 % surface irradiance penetrates, with an optical depth of 4.6.

2.2. Experimental bioassays

For experimental bioassays, water was also collected from the middle of the mixed layer (10-30 m) in 10 L trace-metal free Niskin bottles on a Titanium CTD rosette sampler. Experimental water was then dispensed randomly into 72 individual 4.2 L Nalgene bottles with gas-tight septum and seawater pCO_2 concentrations were modified following Richier et al. (2014). Briefly, the initial carbonate chemistry in the seawater was characterized (see Richier et al., 2014; see also Tarling et al., this issue) and subsequently manipulated in the incubation bottles using an equi-molar addition of strong acid (HCl, 1 mol kg^{-1}) and sodium bicarbonate ($NaHCO_3^-$, 1 mol kg^{-1}) (Gattuso et al., 2010). In addition, three independent bottles were measured immediately after manipulation and checked for the accuracy of the method.

For each treatment (ambient, 550 µatm, 750 µatm and 1000 µatm) there were 18 replicate bottles for measurement of a wide range of chemical, biological and biogeochemical parameters (see Table 3 in Richier et al., 2014) and the measurements for this study came from 6 replicate 4.2 L bottles from each pCO_2 treatment. The microbial communities in each bottle were incubated in a purpose built commercial refrigeration container, with each treatment bottle racked in such a way that no two replicate treatment bottles were incubated alongside one another. Irradiance (100 µmol photons m^{-2} s^{-1}) was provided by daylight simulation LED panels (Powerpax, UK) over a 24 h light cycle, which approximated the ambient photoperiod. Temperature was maintained at the *in situ* values (± 1°C) at the time of water collection by the refrigeration unit and light levels were checked with a 4π scalar PAR irradiance sensor (Biophysical Instruments, QSL-2101). Bioassays were sub-sampled through sacrificial incubation bottles at two time points, the first after 48 h and the second after 96 h. Water samples for PP, total and > 10 µm Chl, BP, C_{bact}, macronutrient concentrations, and particulate silica ($bSiO_2$) were taken from 3 replicate bottles per pCO_2 treatment at both time points. Dissolved inorganic carbon and total alkalinity samples were taken from all experimental bottles at both times points. Samples for the determination of BP were only collected from the ambient and the most extreme pCO_2 treatment (target 1000 µatm), and from 3 replicate bottles per pCO_2 treatment at both times points.

205
206 *2.2. Primary production and production of dissolved organic carbon*
207
208 For *in situ* measurements, water samples were collected in four 70 mL polycarbonate bottles and
209 primary production was measured following Poulton et al. (2014). For the pCO_2 bioassay
210 experiments, individual treatment bottles were sub-sampled into 70 mL polycarbonate bottles from
211 the 4.2 L treatment bottles for each replicate from each pCO_2 treatment (i.e. 3 per pCO_2 treatment).
212 Carbon-14 labelled sodium bicarbonate (925-1739 kBq) was added to each bottle and then three
213 of the bottles were incubated on deck or in the case of samples from the bioassays, samples were
214 incubated in a purpose built constant temperature containerised laboratory (Richier et al., 2014).
215 On deck incubations were carried out in incubators chilled with surface seawater and covered with
216 light filters (Misty-blue and Grey, LEE UK) to replicate 55% of surface irradiance. When surface
217 seawater temperatures were expected to drop sharply (e.g. on entering the Greenland Ice Sheet)
218 *in situ* samples were incubated in the bioassay experimental container. The fourth sample for *in*
219 *situ* measurements had 1 mL of borate buffered formaldehyde added and was incubated in the
220 laboratory and used to measure abiotic uptake. In the case of the pCO_2 bioassay experiments, an
221 average value of the *in situ* abiotic uptake measurement (0.01 mmol C m^{-3} d^{-1}) was subtracted from
222 all the PP rates measured. Production of dissolved organic carbon was measured following López-
223 Sandoval et al. (2011) with the use of 0.2 μm syringe end filtering units (Whatman GD/X Syringe
224 filters with 0.2 μm PTFE membrane) and gentle pressure. Five mL sub-samples were pipetted from
225 each 70 mL incubation bottle into 10 mL syringes and gently filtered through a syringe end filtering
226 unit. Fresh pipette tips, syringes and syringe-end filters were used for each sub-sample to avoid
227 potential contamination.
228
229 Percentage Extracellular Release (PER) was calculated as:
230
231 Percentage Extracellular Release (PER) = 100 x (pDOC / (pDOC + PP)) (1)
232
233 The average relative standard deviation (RSD = Standard deviation/Average x 100) was 16% (1-
234 56%) for total PP, and 35% (2-80%) for pDOC. High RSD for PP was associated with the presence
235 of the colonial haptophyte *Phaeocystis* at several stations (C029, C040) (Le Moigne et al., 2015).
236
237 *2.3. Chlorophyll, macronutrients, particulate silica and carbonate chemistry*
238
239 Total chlorophyll-*a* (Chl) was quantified according to Poulton et al. (2014), with water samples
240 (0.25 L) filtered onto Whatman GF/F filters, extracted in 8 mL 90 % acetone, and stored at 4°C for
241 18-20 h. Fluorescence was measured on a Turner Designs Trilogy fluorometer, calibrated with

purified Chl (Sigma, UK) and drift in the fluorometer was monitored using a solid standard. Chlorophyll in the >10 μm fraction was measured on a 10 μm polycarbonate filter (0.25 L), with Chl in the <10 μm fraction calculated as the difference between total and the >10 μm fraction.

Surface macronutrient (nitrate+nitrite, NOx; phosphate, PO_4; silicic acid, dSi) concentrations were determined using an auto-analyser following standard protocols (Grasshoff et al., 1983). Particulate biogenic silica ($bSiO_2$) measurements were made on 0.5 L seawater samples filtered onto 0.8 μm polycarbonate filters (Nucleopore^{TM}), oven dried (6-8 h, 50^{o}C), and stored dry until samples were digested in 0.2 mol sodium hydroxide, neutralised with 0.1 mol hydrochloric acid, and then analysed using a ATI Unicam 8625 UV/VIS Spectrometer (Ragueneau and Treguer, 1994).

The methodology for dissolved inorganic carbon (C_T) and total alkalinity (A_T) sampling and analysis from CTD samples and experimental samples followed those outlined in Poulton et al. (2014) and Richier et al. (2014) (see also Tynan et al., this issue). Calcite saturation state (Ω_C), pH_T and pCO_2 for both CTD samples and the 96 h bioassay experiments were calculated from C_T, A_T, nutrients, temperature, salinity and pressure data using the CO_2SYS (CO_2 system) program (v. 1.1; Van Heuven et al., 2011) using the carbonic acid dissociation constants of Lueker et al. (2000), the boric acid dissociation constant of Dickson et al. (1990a), the bisulphate ion acidity constant of Dickson et al. (1990b), and boron:chlorinity of Lee et al. (2010).

2.4. Bacterial biomass and bacterial production

Bacterial abundance was assessed with flow cytometry following Zubkov and Burkill (2006), with bacterial biomass estimated using a cellular carbon value of 1.6 fmol C cell^{-1} (Lee and Fuhrman, 1987). Seawater samples (1.6 mL) were preserved with paraformaldehyde (PFA, 1% final concentration) in 2 mL polypropylene screw cap vials, refrigerated and analysed within 12 hours of collection. Samples were stained with SYBR Green I nucleic acid dye and analysed using a FACSort flow cytometer (BD, Oxford) with internal bead standards (Zubkov and Burkill, 2006).

Bacterial production (BP, mmol C m^{-3} d^{-1}) was estimated as the microbial uptake rate of Leucine using carbon-14 labelled leucine (Hartmann Analytic, Germany), added at a concentration of 20 nM, in samples from different depths from each morning CTD. Subsamples of 1.6 mL from each sample were dispensed into 2 mL polypropylene screw cap vials containing carbon-14 leucine (Zubkov et al., 2000). Samples were fixed at each time point (20, 40, 60, and 80 mins) by the addition of 80 µL of 20% PFA (1% v/w final concentration). Fixed samples were filtered onto 0.2 µm polycarbonate membrane filters soaked in non-labelled Leucine solution to reduce abiotic

absorption of radiotracer onto the filters. Filtered samples were washed twice with 4 mL deionised water. Radioactivity of samples was measured as counts per minute (CPM) by liquid scintillation counting (Tri-Carb 3100, Perkin Elmer, UK). Microbial uptake of leucine was computed using specific activity of the Leucine radiotracer.

3. Results

3.1. General oceanography

During the June 2012 cruise, upper ocean (10-30 m) temperatures ranged from -1.6^{o}C to 7.8^{o}C (Table 1), with the lowest temperatures (-1.5^{o}C to -1.6^{o}C) associated with ice shelf conditions in the western Greenland Sea. Mixed layer salinities were also low (<33.3) at the sites associated with the Greenland Ice Shelf (C030, C032, C033), whereas other sampling sites had salinities ranging from 34.6 to 35.2 (Table 1) and were much more indicative of open ocean conditions. The two ice-edge stations (C029, C040) have relatively warm temperatures (3.1-3.5 ^{o}C) and salinities more representative of open ocean sites (~35.0) than those found in the ice (Table 1).

Euphotic zone depths (Z_{eup}) ranged from shallow (21 m) to deep (70 m) across the sampling stations, with deep Z_{eup} (> 50 m) mostly associated with ice conditions in the Greenland Sea (C030, C033) and in the Barents Sea (C047, C052, C054) (Table 1). The shallowest Z_{eup} (< 30 m) were found at two ice-edge stations in the Greenland Sea and Fram Strait (C029, C040, C042). Upper ocean pCO_2 concentrations were variable, ranging from 208 to 381 µatm across the sampling sites with no particular pattern related to the open ocean, ice-edge or ice-sheet sampling sites (Table 1). The highest surface pCO_2 (381 µatm) was at a Greenland Ice Shelf station (C032), whereas the lowest pCO_2 values were associated with a nearby ice-edge station (C029, 209 µatm) and the Fram Strait station (C042, 208 µatm). In a similar way to surface pCO_2, pH_T also varied between sites (range 8.0 to 8.3), though it showed no clear pattern between oceanographic regions (Table 1).

Upper ocean nitrate (NOx) concentrations were generally >6 µmol N kg^{-1} at most sites (Table 1). Three stations had NOx concentrations <4 µmol N kg^{-1}, two across Fram Strait (C029, C042) and one to the north of Iceland (C065), while two stations had NOx <0.6 µmol N kg^{-1} (C019, C047). Phosphate concentrations (not shown) ranged from 0.2 to 0.8 µmol P kg^{-1} and showed a significant ($p<0.001$) correlation with NOx (Pearson's product moment correlation, $r = 0.94$, $n = 21$). The relative concentration of NOx to phosphate, represented here by N* (= NOx - 16*PO_4; e.g. Moore et al., 2009), was low at all sites, as indicated by negative N* values (from -5.8 to -1.2; Table 1). Hence, dissolved inorganic nutrient concentrations were always enriched in phosphate relative to

NOx, with extremely low N* values (less than -2) generally associated with ice influenced areas such as the Greenland Ice Shelf (C029 to C033), Fram Strait (C042) and the northern Barents Sea (C047) (Table 1).

Silicic acid (dSi) concentrations were generally >2 μmol Si kg^{-1} at almost all sampling sites (Table 1), apart from the northern Barents Sea (1.2 μmol Si kg^{-1}, C047). Highest dSi concentrations (>6 μmol Si kg^{-1}) were associated with the Greenland Ice Shelf (C020, C030, C032, C033). Relative to NOx concentrations, dSi concentrations (Si* = dSi - NOx; e.g. Bibby and Moore, 2011) were often high at stations associated with ice influence, as indicated by positive Si* values (Table 1). Conversely, oceanic stations in the Greenland Sea (C020,C021, C027, C060, C063), southern Barents Sea (C052, C054), and Norwegian Sea (C056, C058), all had negative Si* values indicating low dSi relative to NOx concentrations.

Incidental irradiance at the sea surface ($Ed_{[0+]}$) ranged from 19 to 67 mol photons m^{-2} d^{-1} during the June 2012 cruise (Table 1). High values (> 50 mol photons m^{-2} d^{-1}) were experienced at an open ocean station in the Greenland Sea (C020) and at several of the stations associated with the Greenland Ice Shelf (C029, C030, C032). The lowest values (< 25 mol photons m^{-2} d^{-1}) were experienced at stations associated with one of the ice-edge stations (C040), in the northern Norwegian Sea near Svalbard (C045) and in the southern Barents Sea (C052, C054). Most other sampling stations had values between 30 to 40 mol photons m^{-2} d^{-1} (Table 1).

3.2. Total and microplankton chlorophyll a, bacterial biomass and bacterial production

Total Chl ranged from 0.4 to 8.4 mg m^{-3} (average 2.1 mg m^{-3}) in the mixed layer across the sampling sites (Table 2), being highest (>6 mg m^{-3}) at the Iceland-Faroes front (C019) and at one of the ice-edge stations (C029). The in ice stations (C030, C032, C033) all had Chl values <1.5 mg m^{-3}, along with oceanic stations in the Barents (C047, C052, C054), Greenland (C021, C060, C063) and Norwegian seas (CC058), as well as north of Iceland (C065). Microplankton (>10 μm) Chl ranged from 0.02 to 3.1 mg m^{-3} (data not shown), which when expressed as a percentage of total Chl ranged from 2 to 50% (average 21%) (Table 2). High microplankton contributions to Chl (>40% of total) occurred at only two sites, one in the Faroes-Iceland front (C019) and one in the southern Greenland Sea (C063), while low microplankton contributions (<10%) occurred in the Fram Strait (C042), northern Norwegian Sea near Svalbard (C045) and in the Barents Sea (C047, C052, C054). Microplankton Chl ranged from 14-19% at the in ice stations of the Greenland Ice Sheet (C030, C032, C033) and was ~32-34% at the ice-edge stations (C029, C040) (Table 2).

Bacterial biomass (C_{bact}), estimated from flow cytometry counts of bacterial abundance, ranged from 0.5 to 6.4 mmol C m^{-3}, with a cruise average of 2.2 mmol C m^{-3} (Table 2). High C_{bact} (>3 mmol C m^{-3}) was found at sites in the Iceland-Faroes front (C019), Norwegian Sea (C056, C058) and Greenland Sea (C063). Values of C_{bact} were lowest (<1 mmol C m^{-3}) in association with the in ice stations in the Greenland Ice Shelf (C030, C032, C033), Fram Strait (C042) and northern Barents Sea (C047), while the two ice-edge stations (C029, C040) had C_{bact} ~2 mmol C m^{-3}. There was no statistically significant correlation (Pearson's product moment correlation, $p = 0.77$) between total Chl and C_{bact}, whereas there was a significant ($p<0.005$) correlation between C_{bact} and microplankton Chl ($r = 0.635$, $n = 18$).

Bacterial production (BP) ranged from 0.05 to 1.38 mmol C m^{-3} d^{-1}, with a cruise average of 0.28 mmol C m^{-3} d^{-1} (Table 2). A lack of a significant relationship between BP and C_{bact} (Pearson's product moment correlation, $p = 0.16$) resulted in BP showing a different distributional pattern than C_{bact} across the sampling sites. The highest BP (>1 mmol C m^{-3} d^{-1}) was measured in the Faroes-Iceland front (C019), whereas many of the sampling stations had BP rates ~0.2 to 0.4 mmol C m^{-3} d^{-1} (Table 1). Low BP (<0.2 mmol C m^{-3} d^{-1}) occurred at the three in ice stations (C030, C032, C033), the northern Norwegian Sea (C045), southern Barents Sea (C052, C054) and north of Iceland (C065). In contrast to C_{bact}, BP showed significant (Pearson's product moment correlation, $p<0.05$) correlations with both total Chl ($r = 0.51$, $n = 21$) and microplankton Chl ($r = 0.59$, $n = 18$).

3.3. Primary production and production of dissolved organic carbon

Upper ocean rates of primary production (PP) ranged from 0.4 to 5.2 mmol C m^{-3} d^{-1} across the sampling sites (Fig. 2., Table 2). High rates of PP (> 3 mmol C m^{-3} d^{-1}) were found at the Iceland-Faroes front (C019), at the ice-edge of the Greenland Ice Shelf (C029, C040), Fram Strait (C042) and in the Norwegian Sea (C058). Rates of DOC production (*p*DOC) ranged from 0.09 to 0.64 mmol C m^{-3} d^{-1} (Fig. 2), with an average value of 0.26 mmol C m^{-3} d^{-1} for the sampling sites (Table 2). High *p*DOC (>0.4 mmol C m^{-3} d^{-1}) occurred at stations in the Iceland-Faroes front (C019), southern Barents Sea (C054) and southern Greenland Sea (C063) (Fig. 2). Low *p*DOC (<0.1 mmol C m^{-3} d^{-1}) were only measured at two stations, one in the ice (C033) and one across Fram Strait (C042), whereas the majority of sampling sites had values between 0.1 and 0.3 mmol C m^{-3} d^{-1} (Table 2). There were no statistically significant relationships between PP or total Chl and *p*DOC (Pearson's product moment correlation, $p = 0.41$ and $p = 0.73$, $n = 19$, respectively). There was also no significant relationship between PP and C_{bact} (Pearson's product moment correlation, $p = 0.36$, $n = 19$), though there was a significant ($p<0.05$) relationship between PP and BP ($r = 0.53$, $n = 19$).

When expressed as a percentage of total PP, Percentage Extracellular Release (PER) ranged from 2% to 46% (Fig. 2), with a cruise average of 15% (Table 2). The highest values (>30%) of PER were found at two sites in the Barents Sea (C047, C054) while the lower values (<10%) were found at the ice-edge stations (C029, C040), Fram Strait (C042) and in the Norwegian Sea (C056, C058) (Fig. 2). Hence, PER increased in cases where *p*DOC was higher than average and PP was roughly average (e.g., C054), and also when *p*DOC was higher than average and PP was lower than average (C047) (Table 2). There was also a significant ($p<0.05$) inverse correlation between total Chl and PER (Pearson's product moment correlation, $r = -0.48$, $n = 19$). No significant relationships were found between *p*DOC or PER and BP (Pearson's product moment correlation, $p = 0.34$ and $p = 0.55$) or C_{bact} ($p = 0.28$ and $p = 0.52$).

Potential relationships between *p*DOC or PER and the hydrographic parameters described in Table 1 were also examined (Fig. 3). The only significant relationship ($p<0.003$) for *pD*OC was an inverse one with dSi concentration (Pearson's product moment correlation, $r = -0.64$, $p<0.003$, $n = 19$), indicating that *p*DOC increased significantly with decreasing dSi (Fig. 3). For PER, a significant (Pearson's product moment correlation, $p<0.01$) inverse relationship was again found with dSi ($r = -0.55$, $n = 19$), as well as a significant ($p<0.001$) positive relationship with euphotic zone depth (Z_{eup}) (Fig. 3). Hence, for the mixed layer samples, absolute *p*DOC increased with decreasing nutrient (dSi) availability, and when expressed relative to PP, PER increased with increasing euphotic zone depth and decreasing light availability. No significant relationships were observed with SST, absolute nitrate (NOx) or nitrate relative to phosphate (N*), pCO_2, pH_T or incidental irradiance ($Ed_{[0+]}$) (Fig. 3).

3.3. pCO_2 bioassays: macronutrients, primary production and production of dissolved organic carbon

Initial conditions for the three bioassay experiments are given in Table 3 whilst Figure 4 presents the time course of variables in the experiments. The three bioassay experiments were geographically dissimilar in that one (EB-02) was in the sub-polar Iceland Basin, whilst the other two were associated with the Greenland Ice Sheet, one at the ice edge (EB-03) and one in open-water within the ice (EB-04) (Fig. 1A). These geographical variations are clear in the initial starting conditions in terms of hydrographic conditions and initial nutrient concentrations, although the carbonate chemistry of the three (pCO_2, pH_T) was similar (Table 3). One-way Analysis of Variance (ANOVA) tests were used to examine across treatments at each time point (as in Richier et al., 2014).

In the first bioassay experiment (EB-02) there was a general trend for both total Chl and microplankton (>10 µm) Chl to increase, whilst NOx decreased from ~5 µmol N kg^{-1} to ~1 µmol N kg^{-1} (Fig. 4). Although NOx decreased by ~4 µmol N kg^{-1} from the initial value, dSi concentrations and $bSiO_2$ remained at similar levels throughout (~1.5 µmol Si kg^{-1} and ~0.5-0.6 µmol Si kg^{-1}, respectively). In terms of treatment effects, only total Chl showed any significant variability (Fig. 4, $p<0.05$), being around twice as high in the 1000 µatm treatment relative to the others at the mid-time point of the experiment. However, this difference had disappeared by the end time-point. Initial measurements for *p*DOC (and PER) were not made in EB-02 (Fig. 5) so changes from the initiation of the experiment cannot be examined. In EB-02 bacterial production (BP) decreased over the course of the experiment, though showing no difference between treatments (Fig. 5), whereas C_{bact} increased slightly at the mid-time point and then appeared to return to values similar to initial conditions.

In EB-03, both total Chl and >10 µm Chl showed strong increases during the time course of the experiment with total Chl increasing by ~2 mg m^{-3} and >10 µm Chl from <0.5 to almost 3 mg m^{-3} at the end of the experiment (Fig. 4). The sharp increase in >10 µm Chl that occurred between the mid-point and end point in EB-03 resulted in >10 µm Chl representing ~80-90% of the total Chl by the end of the experiment. At the end of EB-03, total Chl in the 750 µatm was significantly higher (Fig. 4, $p<0.05$) than in the other treatments and the 1000 µatm had noticeably lower >10 µm Chl than the other treatments. Initial concentrations of NOx were high in EB-03 compared with the other bioassays (Table 3) and NOx decreased by ~3 µmol N kg^{-1}. Particulate biogenic silica ($bSiO_2$) increased during this bioassay from ~0.5 µmol Si kg^{-1} to 2 µmol Si kg^{-1} which compares reasonably well with the 2 µmol Si kg^{-1} drawdown observed, and also with the strong increase in >10 µm Chl (Fig. 4). No treatment effects were seen in terms of nutrients or $bSiO_2$ in EB-03 (Fig. 4). In the case of *p*DOC in EB-03 there was a notable lack of change in almost all treatments apart from the ambient treatment where it increased (Fig. 5, $p<0.05$). This pattern was also seen in PER (Fig. 5, $p<0.05$), highlighting how PP did not change dramatically across the treatments and showed only a slight increase with time (Fig. 5). BP peaked at the mid-point, being similar at the initial and end point of the experiment, with the difference at the mid-point not being significantly different (Pairwise t-test, $p = 0.167$) (Fig. 5). Bacterial carbon (C_{bact}) decreased dramatically through EB-03 from initial concentrations ~2 mmol C m^{-3}, which were similar to levels seen in EB-02, to <0.5 mmol C m^{-3} at the end. Such a dramatic decrease in C_{bact} was not observed in any of the other experiments and represents a loss rate of C_{bact} of ~0.25 mmol C m^{-3} d^{-1}.

In EB-04, total Chl and >10 µm Chl again showed an increase over time, with an increase in total Chl of ~2 mg m^{-3} and ~4 mg m^{-3} across the experiment (Fig. 4). The high rise in >10 µm Chl in EB-04 resulted in this size fraction representing 80-90% of the total Chl by the end of the experiment.

These increases in Chl were coupled with sharp declines in NOx (from 4 to <1 μmol N kg^{-1}) and dSi (from 12 to 4 μmol N kg^{-1}) and sharp increases in $bSiO_2$ (from 1.5 to 6-9 μmol Si kg^{-1}) (Fig. 4). No significant treatment effects were evident in the nutrient drawdown, with NOx and dSi concentrations depleted to similar extents at the end of the experiment across treatments (Fig. 4). There was also a similar increase in $bSiO_2$ across treatments, with the increase in $bSiO_2$ (~7.5 μmol Si kg^{-1}) matching the drawdown of dSi (~8 μmol Si kg^{-1}) (Fig. 4). Both *p*DOC and PER increased dramatically at the end time point of the experiment relative to the mid-point, although there were no significant treatment effects. As in EB-03, BP in EB-04 peaked at the mid-time point and returned to rates similar to initial ones by the end of the experiment, and there was noticeably higher BP in the 1000 μatm relative to the ambient treatment (Fig. 4). In the case of C_{bact} in EB-04 there was an increase from initial concentrations of ~0.7 mmol C m^{-3} to ~1.5 to >2 mmol C m^{-3}.

Overall, all three bioassay experiments (EB-02, EB-03, EB-04) showed increases in both total Chl and >10 μm Chl, drawdown of NOx and dSi and increases in $bSiO_2$, although the rate of dSi drawdown and magnitude of $bSiO_2$ increase was lowest where initial dSi concentrations were also lowest (EB-02) (Fig. 4, Table 3). Absolute *p*DOC (and PER) showed greater variability between bioassays, showing no change in one, an increase in the ambient in another and a sharp increase in the third (Fig. 5). Bacterial Production (BP) also varied over time and with pCO_2 treatment across the three bioassay experiments, with a decrease in BP in the first bioassay and mid-point peaks in the second and third (Fig. 5). In terms of C_{bact}, the three experiments had completely different patterns: one stayed roughly similar (EB-02), one decreased sharply (EB-03) and one increased (EB-04) (Fig. 5). Clearly slightly different processes occurred across the autotrophic community in the bioassays relative to the heterotrophic components of the community; however no clear treatment effect in terms of pCO_2 was evident in any of the three bioassay experiments.

4. Discussion

4.1. Carbon metabolism of Arctic plankton communities

Although measurements of *p*DOC have been made in the Arctic Ocean in the past (e.g., Gosselin et al., 1997), the use of absorbent glass fibre filters in many of these older studies means that there is uncertainty about the validity of these measurements (Karl et al., 1998). Across our sampling region, from the subpolar Iceland Basin to the Greenland Ice Sheet and polar Barents Sea (Fig. 1), we found a range of net *p*DOC (0.09 to 0.64 mmol C m^{-3} d^{-1}; Table 2) similar to those reported in other marine studies: for example, Marañón et al. (2005) reported net *p*DOC ranging from 0.04 to 0.54 mmol C m^{-3} d^{-1} in the central Celtic Sea in summer, while López-Sandoval et al. (2011) had rates of net *p*DOC of <0.01 to 0.13 mmol C m^{-3} d^{-1} in the Mediterranean Sea.

In terms of PER, our range (2 to 46%) and cruise average (15%) also matches well with multiple studies over many different regions: 5 to 33% in the Southern Ocean (Morán et al., 2002a, 2002b), 6 to 37% in the Mediterranean Sea (Morán et al., 2002a; Lagaria et al., 2013), 7% in the northeast Atlantic, and 4 to 42% in three Atlantic upwelling regions (Benguela, Mauritania and northwest Spain) and the oligotrophic North Atlantic (Teira et al., 2001). Furthermore, our PER values match with the historical study of Gosselin et al. (1997), who found PER to be <20% in the Central Arctic Ocean (Chukichi Sea, Makarov and Nansen Basins).

From our sampling of the Nordic Seas of the Arctic Ocean, the highest rates of *p*DOC (>0.3 to 0.64 mmol C m^{-3} d^{-1}) occurred in the open water post-bloom environments (see Le Moigne et al., 2015) of the Barents and Norwegian Seas and from the Iceland-Faroes Front (Table 2). The ice edge stations (C029, C040) had low rates of *p*DOC and relatively high rates of PP leading to the lowest PER (<5%) measured, with the Fram Strait station showing a similar pattern. The Greenland Ice sheet stations (C030, C032, C033) had moderate levels of *p*DOC and PER ranging from 10-18%, which are not drastically different from many of the other stations sampled. Although the ice edge and ice stations had average levels of *p*DOC and PER, it was noticeable that these stations also had low BP and C_{bact} (Table 2). Generally, stations in the Greenland Ice Shelf and at the ice edge did not show markedly different dynamics in terms of DOC production and only marginally lower levels of heterotrophic activity and biomass.

Spatial trends in *p*DOC (and PER) have been suggested to be linked to gradients in phytoplankton community structure and nutrient availability, so that the release of DOC increases as the community becomes nutrient impoverished and dominated by small cells (Teira et al., 2001, 2003; López-Sandoval et al., 2011). However, studies by Marañón et al. (2004, 2005) in vastly contrasting environments in terms of Chl concentrations, contribution of small cells to total biomass and production, and nutrient availability found very similar PER: 22% for the eutrophic Celtic Sea and 19% for the oligotrophic Ria de Vigo. In our case, *in situ* measurements showed no relationship between *p*DOC and microplankton Chl, although it was noticeable that in EB-04, as diatom biomass increased, *p*DOC also increased (see Section 4.3 for further discussion). Hence, there is little evidence from our observations of a strong influence of community composition on *p*DOC, although we only examine bulk expressions of community composition here (i.e. size-fractionated Chl and particulate silica concentration; Table 2).

The correlation between PP and *p*DOC was not statistically significant (Pearson product moment, $p = 0.180$) and *p*DOC was relatively invariant to variability in PP, although as PP decreased, PER increased. Other studies have observed significant relationships between PP and *p*DOC (e.g.,

Morán et al., 2002b; Marañón et al., 2005; López-Sandoval et al., 2011), while several studies have found, as we found, the opposite (e.g., Teira et al., 2001, 2003). Of these studies, the presence (or lack) of a relationship between *p*DOC and PP is not linked to incubation length, as significant relationships have been found from both short (<6 h) incubations (Morán et al., 2002b) and long (24 h) incubations (Marañón et al., 2005; López-Sandoval et al., 2011). Teira et al. (2001) found a strong relationship between *p*DOC and PP in upwelling nutrient-rich waters and no relationship in nutrient-poor subtropical waters. A positive relationship between PP and *p*DOC may indicate that extracellular release is a major source of DOC rather than trophic interactions (sloppy feeding, viral lysis), whereas a lack of relationship could indicate that extracellular release is less important and/or that there is significant consumption of the released DOC. Indeed, some studies (e.g., Teira et al., 2003) have used these relationships to determine whether the potential sources of DOC were from cellular exudation or trophic interactions. However, due to the potentially rapid utilization of DOC by heterotrophic components of the community and the complex trophic interactions in plankton communities, it would be premature to conclude the source mechanisms using only information on the relationship between PP and net *p*DOC.

Bacterial biomass (C_{bact}) in plankton communities sampled in the Greenland and Norwegian Seas ranged from 0.5 to 6.4 mmol C m^{-3} in this study (Table 2), but did not correlate with total Chl ($p = 0.77$) as observed by Cole et al. (1982). However, there was a statistically significant correlation with microplankton (>10 μm) Chl (Pearson's product moment correlation, $r = 0.635$, $p<0.005$, $n = 18$). Such relationships between large phytoplankton (e.g., diatoms) and heterotrophic biomass potentially indicate stronger coupling of these elements of the ecosystem than seen in other marine environments, which are dominated by small cells.

Phytoplankton biomass (C_{phyto}), estimated from (total) Chl concentrations and a carbon to Chl ratio of 50, ranged from 1.6 to 35 mmol C m^{-3}. When expressed relative to C_{bact}, the ratio of C_{bact}:C_{phyto} ranged from 0.1 to 1.0, with a cruise average of 0.4, indicating that heterotrophic biomass was almost half of that of autotrophic biomass and that there are likely to be strong linkages between the two. In some cases, higher ratios of C_{bact}:C_{phyto} (>0.7) were found in open ocean environments of the Greenland and Norwegian Sea, with these sites likely to be post-bloom summer environments (Le Moigne et al., 2015) with active microbial loops and strong coupling between autotrophic and heterotrophic components of these ecosystems. This conclusion is also supported by a significant (Pearson's product moment correlation, $p<0.01$) inverse relationship between Si* and C_{bact}:C_{phyto} ($r = -0.58$, $n = 19$), indicating that with high NOx:dSi ratios (excess nitrate / depleted silicate) there is stronger coupling.

The ratio of bacterial production (BP) to Primary Production (PP) ranged from 0.1 to 0.9 across the study area, although the cruise average was only 0.2. This cruise average is similar to the average BP to PP ratio (0.3) found across a wide range of marine environments (del Giorgio and Cole, 1998). Only one site had a BP:PP ratio > 0.4 (C047, Barents Sea), and this site also had the lowest PP and nutrient concentrations sampled (Tables 1 and 2), indicating that this site represents an oligotrophic extreme. Variable BP to PP ratios are more indicative of differing degrees of coupling between the autotrophic and heterotrophic components of the ecosystems. The strength of linkage between such components of the ecosystem will critically depend on the characteristics of the dissolved organic matter (including DOC) released from the autotrophs and available for utilization by heterotrophic bacteria, as well as the requirements of the heterotrophs. For example, if the carbon demand for bacterial respiration and growth is met fully or partially by DOC release from phytoplankton.

To examine the degree to which bacterial carbon demand (BCD) was met by the release of DOC, we used the equation of Robinson (2008) to estimate bacterial respiration ($BR = 3.69 \times BP^{0.58}$) and then BCD (= BP + BR) (see also Morán et al., 2002a, b; Teira et al., 2003; López-Sandoval et al. 2011). The average estimate of the *p*DOC contribution to BCD was 16% (range 4% to 43%), with most stations <20%, apart from open ocean stations in the Greenland and Norwegian Seas, which were higher (Table 2). A lack of correlation between rates of DOC release and bacterial activity (BP) and a BCD in excess of *p*DOC suggest the existence of additional organic carbon sources to support bacterial activity (Morán et al., 2002a,b; Teira et al., 2003). Additional DOC sources could include trophic process (zooplankton sloppy feeding, excretion and egestion, cell breakage through viral lysis; Nagata, 2000), as well as possible coastal sources of DOC (Moran et al., 2002a), or in the case of the communities in proximity to the ice sheets, exudation from ice-associated algae.

However, key to the estimation of BCD is knowledge of the bacterial growth efficiency (i.e. the relative amount of carbon invested in new cell production versus that used for respiration), which varies considerably (<5% to 60%, del Giorgio and Cole, 1998; 7% to 69%, García-Martín et al., 2014a; 15% to 65%, Wear et al., 2015), and our understanding of what factors regulate this variability is lacking (del Giorgio and Cole, 1998; Robinson, 2008). For example, studies have contradicted one another in their conclusions about temperature control of bacterial growth efficiency: Rivkin and Legendre (2001) found an inverse relationship, while García-Martín et al. (2014a) found no relationship. Factors determining bacterial growth efficiency may include such things as the metabolic potential and carbon content of the DOC, the taxonomic source and rate of DOC supply, the physiological condition or taxonomy of the bacterial cells, and the ecological or physiological pathways of DOC supply (del Giorgio and Cole, 1998; Fouilland et al., 2014; Wear et al., 2015). This uncertainty in the factors controlling BCD introduces significant uncertainties in

609 estimates of BCD, and hence uncertainty in our conclusion that bacterial communities in the Arctic
610 require alternative sources of DOC rather than the *in situ* plankton to meet their demands.
611
612 *4.2. Ocean Acidification and carbon dynamics in Arctic plankton communities*
613
614 Several previous studies have observed increased release of photosynthetically fixed carbon into
615 the dissolved phase during exposure to elevated CO_2 concentrations under experimental
616 conditions (e.g., Engel, 2002; Czerny et al., 2013; Engel et al., 2013). Such results have been
617 found in mesocosms in sub-polar and polar experiments (e.g., Czerny et al., 2013; Engel et al.,
618 2013), as well as in smaller scale bioassays (e.g., Engel, 2002). Elevated *p*CO2 is believed to lead
619 to 'over consumption' of carbon and a consequent increase in production of DOC and/or
620 transparent exopolymer particles (TEP) (Engel, 2002). A number of studies have also found no
621 change in *p*DOC or PER with experimental increases in pCO_2 (Yoshimura et al., 2010, 2013; Engel
622 et al., 2014; MacGilchrist et al., 2014; Maugendre et al., 2015).
623
624 These previous studies examining the effects of increased pCO_2 and perturbed carbonate
625 chemistry conditions have tended to change pCO_2 conditions over longer timescales (e.g., >4 d,
626 Czerny et al., 2013) than used in this study (<2 h). The pCO_2 manipulation in this study was
627 enforced on the ambient plankton communities within <2 h, which represents a much faster shift in
628 carbonate chemistry than will be experienced with ocean acidification over the next century (see
629 discussion in Richier et al., 2014). Hence, the small-scale bioassays used here tested community
630 sensitivity to sharp changes in carbonate chemistry rather than acclimation or adaptation to OA
631 conditions over weeks (mesocosms), decades or centuries (OA) (Poulton et al., 2014; Richier et
632 al., 2014). Furthermore, previous studies on the effect of pCO_2 changes on DOC release have
633 often enriched their incubations with inorganic nutrients (e.g., Czerny et al., 2013; Engel et al.,
634 2013, 2014) or have retained the original nutrient conditions (e.g., Engel, 2002; Yoshimura et al.,
635 2010, 2013; MacGilchrist et al., 2014; Maugendre et al., 2015). Studies which have observed
636 increased *p*DOC under elevated CO_2 generally measure net *p*DOC (via changes in absolute DOC
637 levels, e.g. Czerny et al., 2013, or over 24 h incubations, Engel et al., 2013), and hence these are
638 not likely to be valid reasons for the differences between our observations and previous studies.
639
640 Given the abrupt changes in carbonate chemistry experienced by ambient plankton communities in
641 our bioassay experiments, we still observed no overall effect of the different pCO_2 treatments on
642 DOC release (Figs. 4 and 5). During the time course of the three bioassay experiments in this
643 study, strong increases in net *p*DOC and PER were only evident in one of the bioassays (EB-04)
644 (Fig. 5) despite the strong increases in Chl (total and >10 μm) and the drawdown of nutrients that
645 occurred in all three bioassays (Fig. 4). Treatment effects, as shown by statistically significant

differences between pCO_2 levels, did occur but showed no clear trend across the three bioassays: for example, total Chl was significantly (one-way ANOVA, $p<0.05$) higher in the 1000 μatm at the mid-point (48 h) in the first bioassay, but not at the end, while significant ($p<0.05$) differences in total Chl were limited to the 750 μatm at the end time point (96 h) in the second bioassay (Fig. 4).

When relative changes in *p*DOC and PER are plotted against changes in pCO_2 (ΔCO_2; between treatment and initial levels) no clear trend of increasing treatment effect with ΔCO_2 is found at either time point in any of the bioassays (Fig. 6). However, when relative changes in *p*DOC and PER are plotted against changes in nutrients (NOx, dSi) between time points and initial concentrations, the third bioassay is clearly different to the other two bioassays with higher relative changes in *p*DOC and PER at nutrient concentrations which are low relative to the initial (Fig. 7). Although the uptake of NOx was similar across the three bioassays (~4 μmol N kg^{-1}), the third bioassay stood out as the one in which NOx levels fell well below 1 μmol N kg^{-1} (Fig. 4). In the case of dSi, the three bioassay experiments were very different (Fig. 4), although EB-04 again stood out as the one in which the largest decline occurred (~8 μmol Si kg^{-1}). Clearly, nutrient availability exerted an influence on the partitioning of production between the particulate and dissolved fractions in our bioassays in the Iceland Basin and Greenland Ice sheet, rather than pCO_2 treatment.

Nutrient availability was also a strong control on *p*DOC and PER in the CTD samples, with statistically significant relationships with declining dSi concentrations (Fig. 3; Pearson's product moment correlation, $r = 0.55$, $p<0.01$, $n = 19$). Increasing Z_{eup} was also associated with increasing PER, though this is partly due to a strong correlation between Z_{eup} and PP ($r = -0.81$, $p<0.001$, $n = 16$). Marañón et al. (2005) found increased PER with increasing depth in the Celtic Sea, which was due to *p*DOC being invariant with depth while PP showed a sharp decrease with depth (i.e. irradiance). This intricate relationship between PP and irradiance is likely to explain partially the relationship between PER and Z_{eup} found in this study. Elevated *p*DOC in the third bioassay (EB-04) could also be related to reduced light availability as the strong increase in biomass occurring in this bioassay could have resulted in self-shading of the phytoplankton community.

Within the bioassay experiments, BCD showed the same trends as BP across the time points, while the proportion of BCD that *p*DOC potentially supplied varied greatly with no obvious pCO_2 treatment effect or with nutrient availability (Table 4). In contrast to the *in situ* measurements, several of the time points in the bioassays had *p*DOC rates that was in excess of BCD (i.e. >100%). This occurred at both pCO_2 levels (ambient and 1000 μatm), but was more often associated with the end time point of the bioassay, while the highest ratios of *p*DOC:BCD (>500%) occurred in the last bioassay (EB-04) when nutrient levels (NOx, dSi) were depleted to ~0.1 μmol

683 N kg^{-1} or below (Table 4, Fig. 4). Such high ratios of *p*DOC to BCD imply that the phytoplankton
684 community was producing more DOC than the bacterial community could utilize, partly due to the
685 strong decreases seen in BP in all three bioassays at the end time point (Fig. 5). Bacterial biomass
686 only decreased in the second bioassay (EB-03), whereas it remained stable (and high) in EB-02
687 and increased to similar levels (~2 mmol C m^{-3}) as EB-02 in EB-04 (Fig. 5). Decreasing BP with
688 little or no change in C_{bact} potentially indicates that the released DOC was being respired and our
689 estimates of bacterial growth efficiency were inaccurate in these cases. It is also possible that the
690 released DOC under conditions of nutrient starvation or rapid algal growth was markedly different
691 in its characteristics (e.g., carbon to mineral stoichiometry; Wear et al., 2015), and caused higher
692 respiration of DOC than that used for new cell growth.
693
694 Of the other parameters measured in the three bioassay experiments (e.g. Chl, $bSiO_2$, C_{bact}; Figs. 4
695 and 5), none showed a clear and repeatable treatment effect. However, similar temporal trends
696 were observed in the three bioassays; for example, there was dSi drawdown in all three bioassays,
697 and comparable increases in $bSiO_2$ also occurred, though the magnitude in each was different
698 (Fig. 4). In a very similar manner to dSi drawdown and $bSiO_2$ production, microplankton Chl also
699 increased across the three bioassays indicating an increasing dominance of large phytoplankton
700 (e.g., diatoms) towards the end of the bioassays.
701
702 *4.3. Is there a role for diatoms as important DOC producers in the Arctic Ocean?*
703
704 Linkages between decreasing dSi availability and increased DOC production from both the *in situ*
705 measurements (Fig. 3) and pCO_2 manipulated bioassays (Figs. 4-7) may indicate that diatoms had
706 a strong role in DOC production in our study. In contrast to the other bioassay experiments, DOC
707 production was high in the EB-04 bioassay at low relative nutrient concentrations compared to
708 initial concentrations (Fig. 7) rather than at increased pCO_2 levels (Fig. 6). The mass balance
709 between dSi drawdown and production of $bSiO_2$ observed in the EB-03 and EB-04 bioassays
710 (across all treatments), as well as the increasing dominance of the >10 μm fraction in terms of Chl
711 (Fig. 4) and primary production (not shown), imply that diatoms became an increasingly dominant
712 component of the autotrophic community in the last two bioassays.
713
714 Simple estimates of diatom carbon, through conversion of $bSiO_2$ using a carbon to silicate ratio of
715 0.13 (Brzezinski, 1985), gives values of diatom carbon ranging from 0.1 to 28.6 mmol C m^{-3}
716 (average 2.8 mmol C m^{-3}). Expressed against C_{phyto}, diatom carbon (C_{dia}) represented 1% to 79%
717 (average 35%) across the Nordic Seas. (Note that this ignores two values >100% from the
718 Norwegian Sea (C058) and north of Iceland (C065), which are indicative that either the assumed
719 carbon to Chl and/or carbon to silica ratio are incorrect for these stations.) In the case of the

bioassays, estimates of C_{dia} give values ranging from 0.7 to 6.6 mmol C m^{-3} and 4.3 to 31.2 mmol C m^{-3} in EB-03 and EB-04 respectively, which equate to 9% to 69% and 38% to >100%, respectively, of estimated C_{phyto}. Hence, diatoms represented a major component of the phytoplankton biomass, and potentially carbon fixation, across the Nordic Seas, implying an importance in DOC production as well as being recognised as having a major role in export of material during summer 2012 (see Le Moigne et al., 2015).

Diatom blooms are potentially large sources of DOC, with rapid DOC release following bloom peak as nutrients (NOx, dSi) are depleted and light availability changes, with selective use of this newly produced DOC by ambient bacteria communities (Norrman et al., 1995; Fouilland et al., 2014). In contrast, Wetz and Wheeler (2007) found high DOC release rates during exponential growth rather than when nutrients were depleted in batch cultures of various coastal diatom species. Also, a study by Fouilland et al. (2014) found significant DOC production from diatom communities and a closer coupling between bacteria and phytoplankton DOC exudation when there was high nutrient availability and low grazing, and small diatoms and autotrophic flagellates dominated the community. Observations in the Santa Barbara Channel (California) by Wear et al. (2015) during seasonal dSi depletion found that DOC concentrations (refractory and labile) both increased, and also that the bacterial growth efficiency increased during the latter stages of the bloom as the characteristics of the dissolved organic matter being released by the plankton community changed. Hence, diatoms and diatom-produced DOC can have a strong influence on DOC dynamics, including the degree of coupling between autotrophic and heterotrophic components of the carbon cycle. Our study therefore indicates a potentially important role of (dSi-starved or light-limited) diatoms in DOC production in the Nordic Seas of the Arctic Ocean.

5. Conclusions

There is a general consensus (e.g., Morán et al., 2002a; Teira et al., 2001, 2003) that the relative importance of *p*DOC increases under strong nutrient limitation, and both our *in situ* and bioassay experiments provide support to this paradigm. The weak coupling between *p*DOC and BCD found in this study, and others (e.g. Morán et al., 2002a, b; López-Sandoval et al., 2011), potentially indicates weak coupling between phytoplankton exudation and bacterial metabolism. This weak coupling implies that in the Nordic Seas other DOC sources (e.g., coastal sources) are required to support bacterial respiratory requirements, which has also been concluded from coastal sites in the Antarctic (Morán et al., 2002a). However, we also note the variability in bacterial growth efficiency, which influences whether DOC supplied to bacteria is respired or used to make new cells, and the current uncertainty in the dominant factors which cause this variability.

In a rapidly changing Arctic climate, with increased sea surface temperatures, decreasing ice coverage and potentially enhanced primary production (Arrigo et al., 2008; Boé et al., 2009; Fabry et al., 2009), our observations have several implications for future work. Firstly, sharp changes in pCO_2 and carbonate chemistry may have little effect on either total carbon fixation or the relative amount of particulate or dissolved phases, although longer term experiments are needed to test the effect of ocean acidification on such communities. Secondly, nutrient (NOx, dSi) and light limitation, through stronger seasonal growth cycles and/or enhanced stratification, could have a strong impact on DOC production, and potential OA effects on plankton communities should be examined in this context in terms of multi-stressors. Lastly, there is a potentially important role of diatoms in PP and DOC production in the Arctic that needs further examination.

Acknowledgements

We acknowledge the UK Natural Environmental Research Council (NERC; Grant references NE/H017097/1 and NE/H017348/1), Department of Environment, Food and Rural Affairs (Defra), and Department of Energy and Climate Change (DECC) for funding the research cruise via the UK Ocean Acidification research programme, and to the Danish, Icelandic and Norwegian diplomatic authorities for granting permission to travel and work in Greenland, Iceland and Svalbard coastal and offshore waters. Two anonymous reviewers are thanked for their constructive comments on a previous draft of the paper.

References

Anderson, L.G., 2002. DOC in the Arctic Ocean. In: Hansell, D.A., Carlson, C.A. (Eds) Biogeochemistry of Marine Dissolved Organic Matter. Academic Press Inc., 665-683.

Arrigo, K.R., van Dijken, G., Pabi, S., 2008. Impact of shrinking Arctic ice cover on marine primary production. Geophys. Res. Lett., 35, L19603.

Boé, J., Hall, A., Qu, X., 2009. September sea-ice cover in the Arctic Ocean projected to vanish by 2100. Nat Geoscience 2, 341-343.

Bibby, T.S., Moore, C.M., 2011. Silicate: nitrate ratios of upwelled waters control the phytoplankton community sustained by mesoscale eddies in sub-tropical North Atlantic and Pacific. Biogeosci. 8, 657-666.

Brzezinski, M.A., 1985. The Si:C:N ratio of marine diatoms: interspecific variability and the effect of some environmental variables. J. Phycol. 21, 347-357.

Cole, J.J., Likens, G.E., Strayer, D.L., 1982. Photosynthetically produced dissolved organic-carbon and important carbon source for planktonic bacteria. Limnol. Oceanogr., 27, 1080-1090.

Czerny, J., Schulz, K.G., Boxhammer, T., Bellerby, R.G.J., Büdenbender, J., Engel, A., Krug, S.A., Ludwig, A., Nachtigall, K., Nondal, G., Niehoff, B., Silyakova, A., Riebesell, U., 2013.

Implications of elevated CO2 on pelagic carbon fluxes in an Arctic mesocosm study - an elemental mass balance approach. Biogeosci., 10, 3109-3125.

Dickson, A. G., 1990a. Thermodynamics of the dissociation of boric acid in synthetic sea water from 273.15 to 318.15 K. Deep-Sea Res., 37, 755-766.

Dickson, A. G., 1990b. Standard potential of the reaction: AgCl(s) + 1/2H_2(g) = Ag(s) + HCl(aq), and the standard acidity constant of the ion HSO_4^- in synthetic seawater from 273.15 to 318.15 K. J. Chem. Thermodyn., 22, 113-127.

del Giorgio, P.A., Cole, J.J., 1998. Bacterial growth efficiency in natural aquatic systems. Annu. Rev. Ecol. Syst., 29, 503-541.

Engel, A., 2002. Direct relationship between CO_2 uptake and transparent exopolymer particles production in natural phytoplankton. Deep-Sea Res. 24(1), 49-53.

Engel, A., Delille, B., Jacquet, S., Riebesell, U., Rochelle-Newall, E., Terbrüggen, A., Zondervan, I., 2004. Transparent exopolymer particles and dissolved organic carbon production by *Emiliania huxleyi* exposed to different CO_2 concentrations: a mesocosm experiment. Aquatic Microbial Ecol. 34, 93-104.

Engel, A., Borchard, C., Piontek, J., Schulz, K.G., Riebesell, U., Bellerby, R., 2013. CO_2 increases ^{14}C primary production in an Arctic plankton community. Biogeosciences 10, 1291-1308.

Engel, A., Piontek, J., Grossart, H.-P., Riebesell, U., Schulz, K.G., Sperling, M., 2014. Impact of CO_2 enrichment on organic matter dynamics during nutrient induced coastal phytoplankton blooms. J. Plankton Res. 36(3), 641-657.

Fabry, V.J., McClintock, J.B., Mathis, J.T., Grebmeier, J.M., 2009. Ocean acidification at high latitudes: The bellwether. Oceanography 22, 161-171.

Fouilland, E., Tolosa, I., Bonnet, D., Bouvier, C., Bouvier, T., Bouvy, M., Got, P., Le Floc'h, E., Mostajir, B., Roques, C., Sempéré, R., Sime-Ngando, T., Vidussi, F., 2014. Bacterial carbon dependence on freshly produced phytoplankton exudates under different nutrient availability and grazing pressure conditions in coastal marine waters. FEMS Microbial Ecol. 87, 757-769.

García-Martín, E.E., McNeill, S., Serret, P., Leakey, R.J.G., 2014a. Plankton metabolism and bacterial growth efficiency in offshore waters along a latitudinal transect between the UK and Svalbard. Deep-Sea Res. I 92, 141-151.

García-Martín, E.E., Serret, P., Leakey, R.J.G., 2014b. Plankton community and bacterial metabolism in Arctic sea ice leads during summer 2010. Deep-Sea Res. I. 92, 152-161.

Gattuso, J.-P., Lee, K., Rost, B., Schulz, K., Gao, K., 2010. Approaches and tools to manipulate the carbonate chemistry, in: Guide to best practices for ocean acidification research and data reporting, Riebesell, U., Fabry, V.J., Hansson, L., Gattuso, J.-P. (eds). Luxembourg, Publications Office of the European Union.

Gosselin, M., Levasseur, M., Wheeler, P.A., Horner, R.A., Booth, B.C., 1997. New measurements of phytoplankton and ice algal production in the Arctic Ocean. Deep-Sea Res. II 44, 1623-1644.

Grasshoff, K., Ehrhardt, M., Kremling, K., 1983. Methods of seawater analysis. Weinhem, Verlag Chemie.

Hansell, D.A., 2002. DOC in the global ocean carbon cycle. In: Hansell, D.A., Carlson, C.A. (Eds) Biogeochemistry of Marine Dissolved Organic Matter. Academic Press Inc., 685-715.

Hansell, D.A., Carlson, C.A., 2015. DOM sources, sinks, reactivity and budgets, p. 65-126. In: Hansell, D.A., Carlson, C.A. (eds), Biogeochemistry of marine dissolved organic matter, 2nd edition, Academic Press.

Karl, D.M., Hebel, D.V., Bjorkman, K., Letelier, R.M., 1998. The role of dissolved organic matter release in the productivity of the oligotrophic North Pacific Ocean. Limnol. Oceanogr., 43, 1270-1286.

Kiørbe, T., 1993. Turbulence, phytoplankton cell size, and the structure of the pelagic food webs. Adv. Mar. Biol., 29, 1-72.

Lagaria, A., Psarra, S., Gogou, A., Tuğrul, S., Christaki, U., 2013. Particulate and dissolved primary production along a pronounced hydrographic and trophic gradient (Turkish Straits System-NE Aegean Sea). J. Mar. Sys. 119-120, 1-10.

Le Moigne, F.A.C., Poulton, A.J., Henson, S.A., Daniels, C.J., Fragoso, G.M., Mitchell, E., Richier, S., Russell, B.C., Smith, H.E.K., Tarling, G.A., Young, J.R., Zubkov, M., 2015. Carbon export efficiency and phytoplankton community composition in the Atlantic sector of the Arctic Ocean. J. Geophys. Res., in press.

Lee, K., Kim, T.-W., Byrne, R. H., Millero, F. J., Feely, R. A., Liu, Y.-M., 2010. The universal ratio of boron to chlorinity for the North Pacific and North Atlantic oceans. Geochimica et Cosmochim. Acta, 74, 1801-1811.

Lee, S., Fuhrman, J.A., 1987. Relationships between biovolume and biomass of naturally derived marine bacterioplankton. Applied. Env. Microbiol. 53(6), 1298-1303.

López-Sandoval, D.C., Fernández, A., Marañón, E., 2011. Dissolved and particulate primary production along a longitudinal gradients in the Mediterranean Sea. Biogeosciences 8, 815-825.

Lueker, T. J., Dickson, A. G., Keeling, C. D., 2000. Ocean pCO_2 calculated from dissolved inorganic carbon, alkalinity, and equations for K_1 and K_2: validation based on laboratory measurements of CO_2 in gas and seawater at equilibrium. Mar. Chem., 70, 1801-1811.

MacGilchrist, G.A., Shi, T., Tyrrell, T., Richier, S., Moore, C.M., Dumousseaud, C., Achterberg, E.P., 2014. Effect of enhanced pCO_2 levels on the production of dissolved organic carbon and transparent exopolymer particles in short-term bioassay experiments. Biogeosci., 11, 3695-3706.

Marañón, E., Cermeño, P., Fernández, E., Rodríguez, J., Zabala, L., 2004. Significance and mechanisms of photosynthetic production of dissolved organic matter in a coastal eutrophic ecosystem. Limnol. Oceanogr., 49, 1652-1666.

867 Marañón, E., Cermeño, P., Pérez, V., 2005. Continuity in the photosynthetic production of
868 dissolved organic carbon from eutrophic to oligotrophic waters. Mar. Ecol. Prog. Ser. 299, 7-17.
869 Maugendre, L., Gattuso, J.-P., Poulton, A.J., Dellisanti, W., Gaubert, M., Guieu, C., Gazeau, F.,
870 2015. No detectable effect of ocean acidification on the plankton metabolism in the north west
871 Mediterranean Sea: results from two mesocosm studies. Estuarine, Coastal and Shelf Science,
872 in press.
873 Moore, C.M., Mills, M.M., Achterberg, E.P., Geider, R.J., LaRoche, J., Lucas, M.I., McDonagh,
874 E.L., Pan, X., Poulton, A.J., Rijkenberg, M.J.A., Suggett, D.J., Ussher, S.J., Woodward, E.M.S.,
875 2009. Large-scale distribution of Atlantic nitrogen fixation controlled by iron availability. Nat.
876 Geosci. 2, 867-871.
877 Morán, X.A.G., Estrada, M., Gasol, J.M., Pedrós-Alió, C., 2002a. Dissolved primary production and
878 the strength of phytoplankton bacterioplankton coupling in contrasting marine regions. Microb.
879 Ecol., 44, 217-223.
880 Morán, X.A.G., Gasol, J.M., Pedrós-Alió, C., Estrada, M., 2002b. Dissolved and particulate primary
881 production and bacterial production in offshore Antarctic waters during austral summer: coupled
882 or uncoupled? Mar. Ecol. Prog. Ser. 222, 25-39.
883 Nagata, T., 2000. Production mechanisms of dissolved organic matter. In: Kirchman, D.L. (ed)
884 Microbial ecology of the oceans. John Wiley & Sons, Chichester, p 121-152.
885 Norrman, B., Zweifel, U.L., Hopkinson, C.S., Fry, B., 1995. Production and utilization of dissolved
886 organic carbon during an experimental diatom bloom. Limnol. Oceanogr. 40, 898-907.
887 Poulton, A.J., Stinchcombe, M.C., Achterberg, E.P., Bakker, D.C.E., Dumousseaud, C., Lawson,
888 H.E., Lee, G.A., Richier, S., Suggett, D.J., Young, J.R., 2014. Coccolithophores on the north-
889 west European shelf: calcification rates and environmental controls. Biogeosci., 11, 3919-3940.
890 Ragueneau, O., Treguer, P., 1994. Determination of silica in coastal waters - applicability and limits
891 of the alkaline digestion method. Mar. Chem. 45, 43-51.
892 Richier, S., Achterberg, E.P., Dumousseaud, C., Poulton, A.J., Suggett, D.J., Tyrrell, T., Zubkov,
893 M.V., Moore, C.M., 2014. Carbon cycling and phytoplankton responses within highly-replicated
894 shipboard carbonate chemistry manipulation experiments conducted around north-west
895 European shelf seas. Biogeosci., 11, 4733-4752.
896 Rivkin, R.B., Legendre, L., 2001. Biogenic carbon cycling in the upper ocean: effects of microbial
897 respiration. Science 291, 2398-2400.
898 Robinson, C., 2008. Heterotrophic bacterial respiration. In: Kirchman, DL (Ed) Microbial Ecology of
899 the Oceans. John Wiley and Sons, Inc. 299-334.
900 Royal Society, 2005. Ocean acidification due to increasing atmospheric carbon dioxide. The Royal
901 Society, London.

902 Tarling, G.A., Peck, V., Ward, P., Ensor, N., Achterberg, E.A., Tynan, E., Poulton, A.J., Zubkov,
903 M.V., Leakey, R.J., 2015. Effects of ocean acidification on polar planktonic food webs – a
904 spatially-extensive microcosm approach. Deep-Sea Res., this issue.
905 Teira, E., Pazó, M.J., Serret, P., Fernández, E., 2001. Dissolved organic carbon production by
906 microbial populations in the Atlantic Ocean. Limnol. Oceanogr. 46, 1370-1377.
907 Teira, E., Pazo, M.J., Quevedo, M., Fuentes, M.V., Niell, F.X., Fernandez, E., 2003. Rates of
908 dissolved carbon production and bacterial activity in the eastern North Atlantic Subtropical Gyre
909 during summer. Mar. Ecol. Prog. Ser. 249, 53-67.
910 Tynan, E., Ribas-Ribas, M., Clarke, J.S., Humphreys, M.P., Rerolle, V.M.C., Esposito, M., Thorpe,
911 S.E., Tyrrell, T., Achterberg, E.P. (this issue). Physical and biogeochemical controls on the
912 variability in surface carbonate chemistry in the Arctic and Southern Oceans. Deep-Sea
913 Research II.
914 Van Heuven, S., Pierrot, D., Rae, J. W. B., Lewis, E., Wallace, D. W. R., 2011. CO2SYS v 1.1,
915 MATLAB program developed for CO_2 system calculations. ORNL/CDIAC-105b. Carbon Dioxide
916 Information Analysis Center, O. R. N. L., U.S DoE, Oak Ridge, TN (Ed.).
917 Wear, E.K., Carlson, C.A., James, A.K., Brzezinski, M.A., Windecker, L.A., Nelson, C.E., 2015.
918 Synchronous shifts in dissolved organic carbon bioavailability and bacterial community
919 responses over the course of an upwelling-driven phytoplankton bloom. Limnol. Oceanogr. 60,
920 657-677.
921 Wetz, M.S., Wheeler, P.A., 2007. Release of dissolved organic matter by coastal diatoms. Limnol.
922 Oceanogr. 52(2), 798-807.
923 Yoshimura, T., Niskioka, J., Suzuki, K., Hattori, H., Kiyosawa, H., Watanabe, Y.W., 2010. Impacts
924 of elevated CO2 on organic carbon dynamics in nutrient depleted Okhotsk Sea surface waters.
925 J. Exp. Mar. Biol. Ecol. 395, 191-198.
926 Yoshimura, T., Suzuki, K., Kiyosawa, H., Ono, T., Hattori, H., Kuma, K., Nishioka, J., 2013.
927 Impacts of elevated CO_2 on particulate and dissolved organic matter production: microcosm
928 experiments using iron-deficient plankton communities in open subarctic waters. J. Oceanogr.
929 69, 601-618.
930 Zubkov, M.V., Burkill P.H., 2006. Syringe pumped high speed flow cytometry of oceanic
931 phytoplankton. Cytometry Part A, 69, 1010-1019.
932 Zubkov, M.V., Sleigh, M.A., Burkill, P.H., Leakey, R.J.G., 2000. Bacterial growth and grazing loss
933 in contrasting areas of North and South Atlantic. J. Plankt. Res. 22, 685-711.

TABLE LEGENDS

Table 1. Oceanographic characteristics of the sampling stations, including CTD number, date sampled, latitude and longitude, sampling location, sampling depth, surface temperature, salinity, euphotic zone depth (Z_{eup}), pCO_2, pH, nitrate (NOx) and silicic acid (dSi) concentration, nitrate to phosphate ratio (N*), silicate to nitrate ratio (Si*) and incidental irradiance ($Ed_{[0+]}$).

Table 2. Surface biogeochemistry of sampling stations, including CTD number, sampling location, total and microplankton (>10 μm) chlorophyll (Chl), primary production (PP), DOC production (*p*DOC), percentage extracellular release (PER), bacterial production (BP), bacterial carbon demand (BCD), ratio of *p*DOC to BCD, bacterial biomass (C_{bact}) and particulate silica ($bSiO_2$). a indicates in situ sample incubated in temperature controlled refrigerated container rather than on-deck (see methods). Standard deviations are given in brackets for *p*DOC and PP.

Table 3. Average initial conditions for the three bioassay experiments. Standard errors are given in brackets.

Table 4. Average values of estimated bacterial carbon demand (BCD) in pCO_2 manipulation experiments for ambient and 1000 μatm treatments. Standard errors are given in brackets. NA indicates not available.

Table 1.

CTD	Date	Lat. [°N]	Long. [°W]	Location	Depth [m]	Temp. [°C]	Salinity	Z_{eup} [m]	pCO_2 [µatm]	pH	NOx [µmol kg^{-1}]	dSi	N*	Si*	$Ed_{[0+]}$ [mol photons m^{-2} d^{-1}]
C019	10 Jun	65.59°N	10.43°W	Iceland - Faroes Front (N)	24	3.6	34.8	32	240	8.2	0.6	2.5	-3.0	1.9	34
C020	11 Jun	69.54°N	07.35°W	Greenland Sea (S)	15	3.1	35.0	38	363	8.1	9.1	6.1	-1.2	-3.0	53
C021	12 Jun	74.07°N	04.42°W	Greenland Sea (C)	15	1.0	34.9	60	308	8.1	9.8	5.7	-1.4	-4.0	40
C027	13 Jun	76.11°N	02.33°W	Greenland Sea (N)	20	1.5	34.9	ND	319	8.1	9.3	4.7	-1.4	-4.6	42
C029	14 Jun	78.43°N	-00.00°E	Ice edge	10	3.5	35.0	21	209	8.3	2.6	5.5	-2.4	2.9	51
C030	15 Jun	78.15°N	05.33°W	Ice	20	-1.6	33.3	53	277	8.2	7.6	6.4	-5.8	-1.2	67
C032	16 Jun	78.13°N	05.60°W	Ice	10	-1.5	32.5	ND	381	8.0	6.6	8.0	-3.7	1.5	51
C033	17 Jun	77.49°N	04.58°W	Ice	14	-1.6	33.0	66	350	8.1	6.4	7.0	-2.4	0.6	38
C040	19 Jun	77.51°N	01.18°W	Ice edge	15	3.1	34.9	28	309	8.1	8.7	5.6	-1.2	-3.1	20
C042	20 Jun	78.59°N	-07.59°E	Fram Strait	15	6.0	35.1	22	208	8.3	4.0	4.3	-2.1	0.4	28
C045	22 Jun	76.16°N	-12.32°E	Norwegian Sea (N)	20	5.7	35.2	39	309	8.1	9.8	5.8	-1.8	-4.0	19
C047	23 Jun	76.09°N	-26.04°E	Barents Sea (N)	25	1.5	34.6	70	238	8.2	0.2	1.2	-2.7	1.0	27
C052	24 Jun	72.53°N	-26.00°E	Barents Sea (S)	15	6.5	35.0	67	324	8.1	7.8	4.4	-1.2	-3.4	20
C054	25 Jun	71.45°N	-17.54°E	Barents Sea (S)	13	7.8	35.0	62	320	8.1	6.0	3.8	-1.8	-2.2	24
C056	26 Jun	71.45°N	-08.27°E	Norwegian Sea (C)	15	6.7	35.2	32	305	8.1	6.8	5.2	-1.2	-1.6	33
C058	27 Jun	71.45°N	01.16°W	Norwegian Sea (C)	20	5.4	35.1	ND	316	8.1	10.6	5.7	-1.7	-4.9	35
C060	28 Jun	71.45°N	10.36°W	Greenland Sea (S)	26	1.4	34.7	55	328	8.1	8.6	2.2	-1.6	-6.5	49
C063	29 Jun	68.42°N	10.35°W	Greenland Sea (S)	20	3.8	34.8	43	318	8.1	8.9	2.6	-1.5	-6.3	40
C065	30 Jun	67.50°N	16.25°W	Iceland (N)	20	5.1	34.9	48	246	8.2	4.0	4.1	-2.8	0.0	33

Table 2.

CTD	Location	Total Chl [mg m^{-3}]	>10 μm Chl [%]	PP [mmol C m^{-3} d^{-1}]	*p*DOC [mmol C m^{-3} d^{-1}]	PER [%]	BP [mmol C m^{-3} d^{-1}]	BCD [mmol C m^{-3} d^{-1}]	*p*DOC/BCD [%]	C_{bact} [mmol C m^{-3}]	$bSiO_2$ [mmol Si m^{-3}]
C019	Iceland - Faroes Front (N)	6.2	50	3.7 (0.1)	0.44 (0.20)	11	1.38	5.8	8	3.8	1.1
C020	Greenland Sea (S)	2.1	31	1.1 (0.2)	0.21 (-)	16	0.16	1.4	15	1.7	0.2
C021	Greenland Sea (C)	0.7	20	0.9 (0.1)	0.18 (0.08)	17	0.23	1.8	10	2.4	0.3
C027	Greenland Sea (N)	1.3		2.2 (0.1)	0.16 (0.01)	7	0.19	1.6	10	1.6	0.4
C029	Ice edge	8.4	32	3.8 (0.3)a	0.17 (0.04)a	4[a]	0.36	2.4	7	1.8	0.7
C030	Ice	1.0	14	1.1 (0.1)	0.24 (0.09)	18	0.11	1.1	22	0.6	0.2
C032	Ice	0.5	19	0.8 (0.1)	0.15 (0.07)	16	0.07	0.8	18	0.5	0.2
C033	Ice	0.5	15	0.9 (0.2)	0.10 (0.00)	10	0.05	0.7	14	0.5	0.7
C040	Ice edge	3.1	34	5.2 (0.5)	0.21 (0.02)	4	0.48	2.9	7	1.9	
C042	Fram Strait	4.3	5	3.9 (0.8)	0.09 (0.01)	2	0.30	2.1	4	0.9	0.4
C045	Norwegian Sea (N)	2.0	8	1.8 (0.4)	0.24 (0.14)	12	0.13	1.3	19	2.0	0.2
C047	Barents Sea (Ice)	0.4	5	0.4 (0.0)	0.34 (0.09)	46	0.35	2.4	14	0.5	0.1
C052	Barents Sea (S)	1.3	2	1.5 (0.3)	0.33 (0.20)	18	0.12	1.2	28	1.8	<0.1
C054	Barents Sea (S)	1.0	6	1.5 (0.2)	0.64 (0.52)	30	0.17	1.5	43	2.2	0.3
C056	Norwegian Sea (C)	2.0	37	2.3 (1.2)	0.17 (0.10)	7	0.20	1.6	10	6.4	0.2
C058	Norwegian Sea (C)	1.0		3.9 (0.2)	0.15 (0.04)	4	0.36	2.4	6	3.0	0.6
C060	Greenland Sea (S)	1.5	23	1.1 (1.2)	0.33 (0.16)	23	0.27	2.0	16	2.8	0.4
C063	Greenland Sea (S)	1.3	43	1.6 (0.3)	0.48 (0.11)	23	0.27	2.0	24	5.2	0.2
C065	Iceland (N)	0.8	18	1.4 (0.2)	0.39 (0.02)	22	0.11	1.1	34	1.2	3.7
	MEAN	2.1	21	2.1	0.26	15	0.28	1.9	16	2.2	0.6
	MIN	0.4	2	0.4	0.09	2	0.05	0.7	4	0.5	<0.1
	MAX	8.4	50	5.2	0.64	46	1.38	5.8	23	6.4	3.7

961 **Table 3.**

962

Parameter	EB02	EB03	EB04
Location	Iceland Basin	Ice Edge	Greenland Ice Sheet
Latitude	60° 35.62'N	76° 10.51'N	78° 21.15'N
Longitude	018° 51.39'W	002° 32.96'W	003° 39.85'W
pCO_2 (µatm)	310 [7]	289 [10]	305 [0.3]
pH_T	8.14 [0.01]	8.16 [0.02]	8.13 [0.01]
SST (°C)	10.62 [0.06]	1.68 [0.01]	-1.57 [0.04]
Salinity	35.2 [0.0]	34.9 [0.0]	32.6 [0.0]
Nitrate (µmol N kg^{-1})	5.02 [0.09]	9.52 [0.50]	4.19 [0.17]
Silicic acid (µmol Si kg^{-1})	1.56 [0.18]	3.77 [0.32]	10.30 [0.03]

963

964

965 **Table 4.**

966

Bioassay	Treatment	Time point	BCD [mmol C m^{-3} d^{-1}]	pDOC/BCD [%]	NOx [μmol N kg^{-1}]
EB02	Initial	T_0	0.96 [0.06]	NA	5.0 [0.1]
	Ambient	T_{48}	0.81 [0.08]	41 [13]	3.5 [0.3]
	Ambient	T_{96}	0.43 [0.05]	81 [10]	1.6 [0.5]
	1000 μatm	T_{48}	0.82 [0.06]	86 [23]	3.6 [0.1]
	1000 μatm	T_{96}	0.41 [0.01]	159 [54]	1.7 [0.2]
EB03	Initial	T_0	0.45 [0.03]	34 [6]	9.3 [0.1]
	Ambient	T_{48}	1.19 [0.25]	21 [13]	8.6 [0.1]
	Ambient	T_{96}	0.21 [0.02]	456 [123]	6.7 [0.1]
	1000 μatm	T_{48}	1.97 [0.39]	7 [1]	8.5 [0.1]
	1000 μatm	T_{96}	0.33 [0.03]	33 [11]	6.9 [0.2]
EB04	Initial	T_0	0.36 [0.02]	59 [29]	4.2 [0.2]
	Ambient	T_{48}	1.26 [0.00]	29 [<1]	1.3 [0.3]
	Ambient	T_{96}	0.60 [0.01]	545 [59]	0.1 [<0.1]
	1000 μatm	T_{48}	1.62 [0.29]	13 [2]	1.3 [0.5]
	1000 μatm	T_{96}	0.74 [0.12]	510 [236]	<0.1 [<0.1]

967

FIGURE LEGENDS

Fig. 1. Cruise track and sampling locations for field samples (circles) and bioassay experiments (stars) superimposed on composite (June 2012) satellite images of (A) sea ice extent (in blue) and topography, and (B) MODIS sea surface temperature. Sea ice concentration data from the Nimbus-7 SMMR and DMSP SSM/I-SSMIS passive microwave sensors were obtained from the National Snow and Ice Data Centre (www.nsidc.org). MODIS sea surface temperature data were obtained from the NASA Ocean Color distributed archive (http: //oceancolor.gsfc.gov/). Numbers in A indicate CTD positions (see Table 1).

Fig. 2. Surface rates. (A) Primary production (PP), (B) DOC production (*p*DOC), and (C) Percentage Extracellular Release (PER). Error bars are standard deviations (n = 3) from *in situ* measurements.

Fig. 3. Scatter plots of DOC production (*p*DOC, A-H) and percentage extracellular release (PER, I-P) against environmental factors: (A, I) Sea-surface temperature (SST, ^{o}C); (B, J) Nitrate+nitrite concentration (NOx, μmol N kg^{-1}); (C, K) Ratio of nitrate(+nitrite) to phosphate as represented by N*; (D, L) Silicic acid concentration (dSi, μmol Si kg^{-1}); (E, M) In situ partial pressure of CO_2 (pCO_2, μatm); (F, N) pH_T; (G, O) Depth of the euphotic zone (Z_{eup}, m); (H, P) Incidental irradiance ($Ed_{[0+]}$, mol photons m^{-2} d^{-1}). Pearson-product moment correlation coefficients (r) are given for significant ($p < 0.05$) correlations.

Fig. 4. Time series measurements of total chlorophyll (TChl, mg m^{-3}), >10 μm chlorophyll (>10 μm Chl, mg m^{-3}), NOx (μmol N kg^{-1}), silicic acid (dSi, μmol Si kg^{-1}) and particulate silica ($bSiO_2$, μmol Si kg^{-1}) for the three pCO_2 bioassays (EB-02, EB-03, EB-04). Plotted values are means ± standard errors (se) from triplicate sample bottles per treatment. Observation of any statistically significant differences between treatments (1-way ANOVA, $p < 0.05$) for each variable and time point are indicated by *.

Fig. 5. Time series measurements of dissolved organic carbon (DOC) production (*p*DOC, mmol C m^{-3} d^{-1}), primary production (PP, mmol C m^{-3} d^{-1}), percentage extracellular release (PER, %), bacterial production (BP, mmol C m^{-3} d^{-1}) and heterotrophic bacteria biomass (C_{bact}, mmol C m^{-3}) for the three pCO_2 experiments (EB-02, EB-03, EB-04). Plotted values are means ± se from triplicate sample bottles per treatment. Observation of any statistically significant differences between treatments (1-way ANOVA, $p < 0.05$) for each variable and time point are indicated by *.

Fig. 6. Relative changes in (a,c) dissolved organic carbon (DOC) production (*p*DOC) and (b,d) percentage extracellular release (PER) for two time points in pCO_2 experiments (T_{48}: a,b; T_{96}: c,d). Errors bars are standard deviations across triplicate treatment bottles.

Fig. 7. Relative changes in dissolved organic carbon production (*p*DOC) and percentage extracellular release against (a, c) NOx (nitrate+nitrite) drawdown and (b, d) silicic acid (dSi) drawdown in the three bioassay experiments. Errors bars are standard deviations across triplicate treatment bottles.

Figure(s)

Figure 1

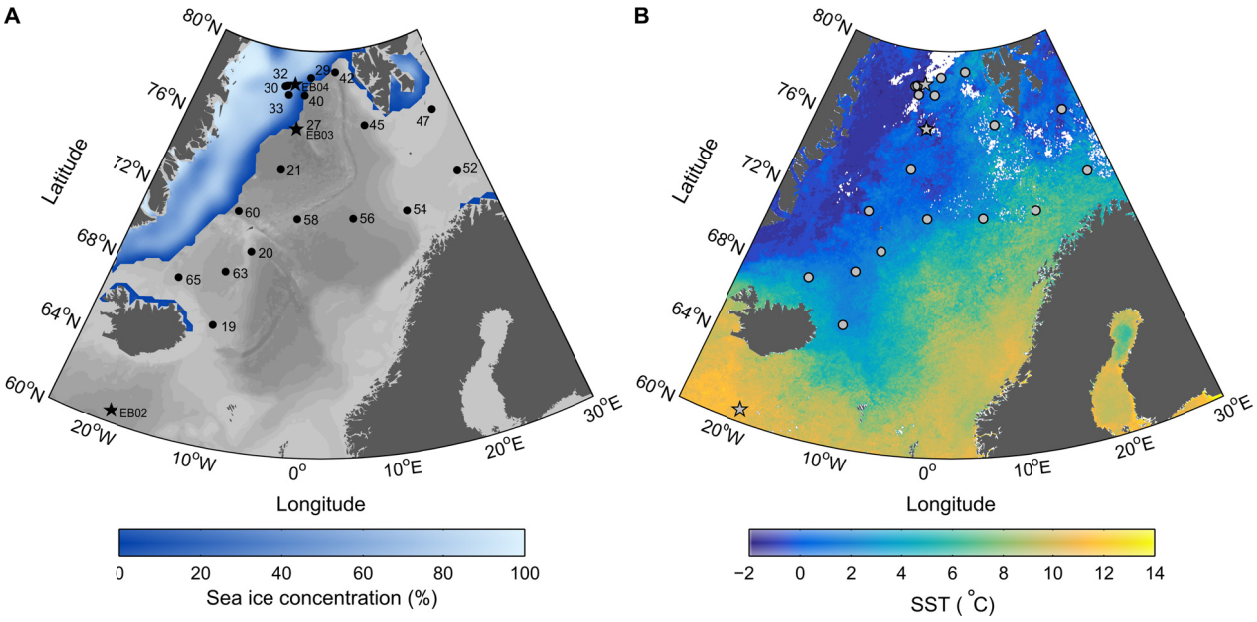

Figure 2

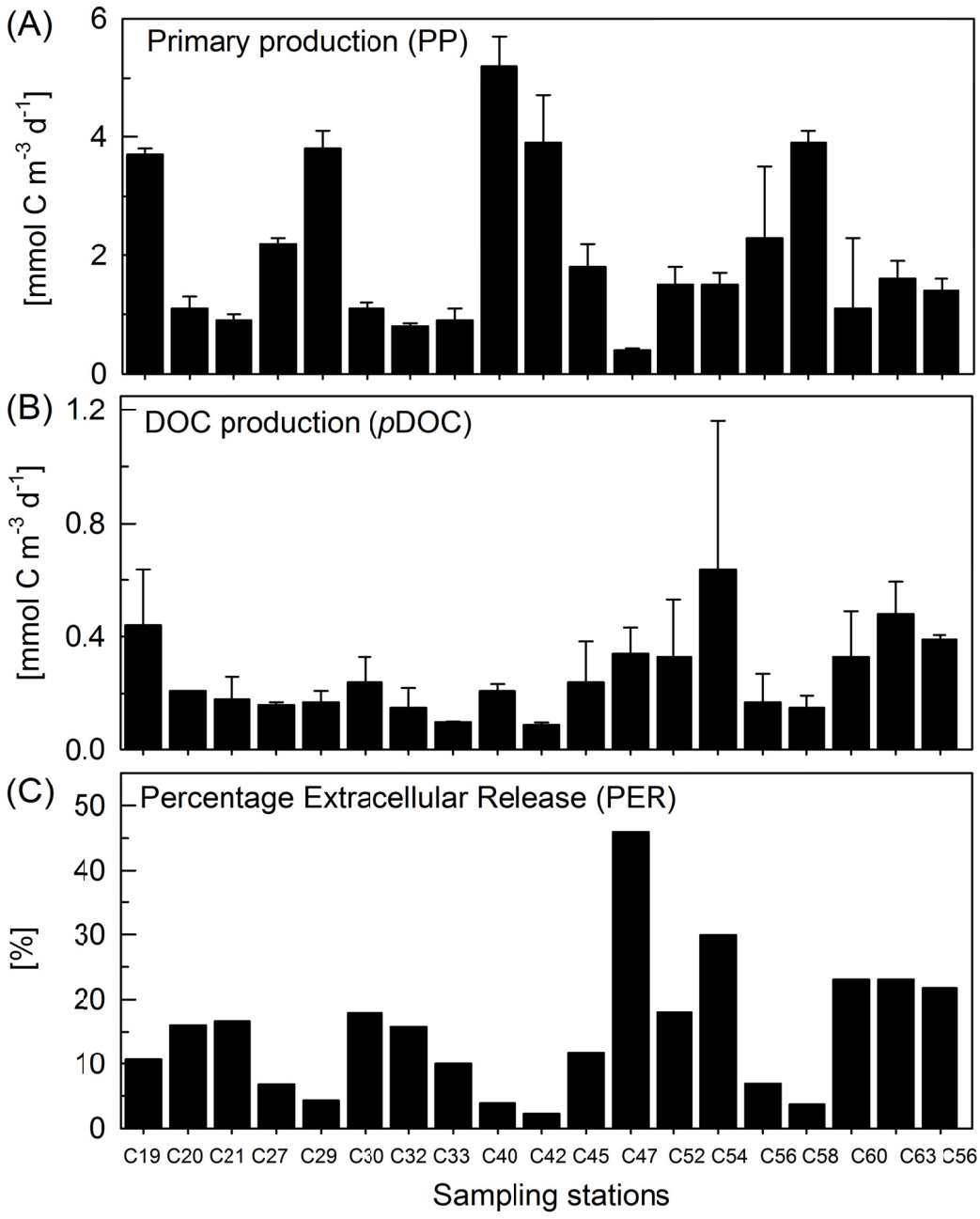
(A)
Primary production (PP)
[mmol C m-3 d-1]
6
4
2
0
(B)
DOC production (pDOC)
[mmol C m-3 d-1]
1.2
0.8
0.4
0.0
(C)
Percentage Extracellular Release (PER)
[%]
50
40
30
20
10
0
C19 C20 C21 C27 C29 C30 C32 C33 C40 C42 C45 C47 C52 C54 C56 C58 C60 C63 C56
Sampling stations

Figure 3

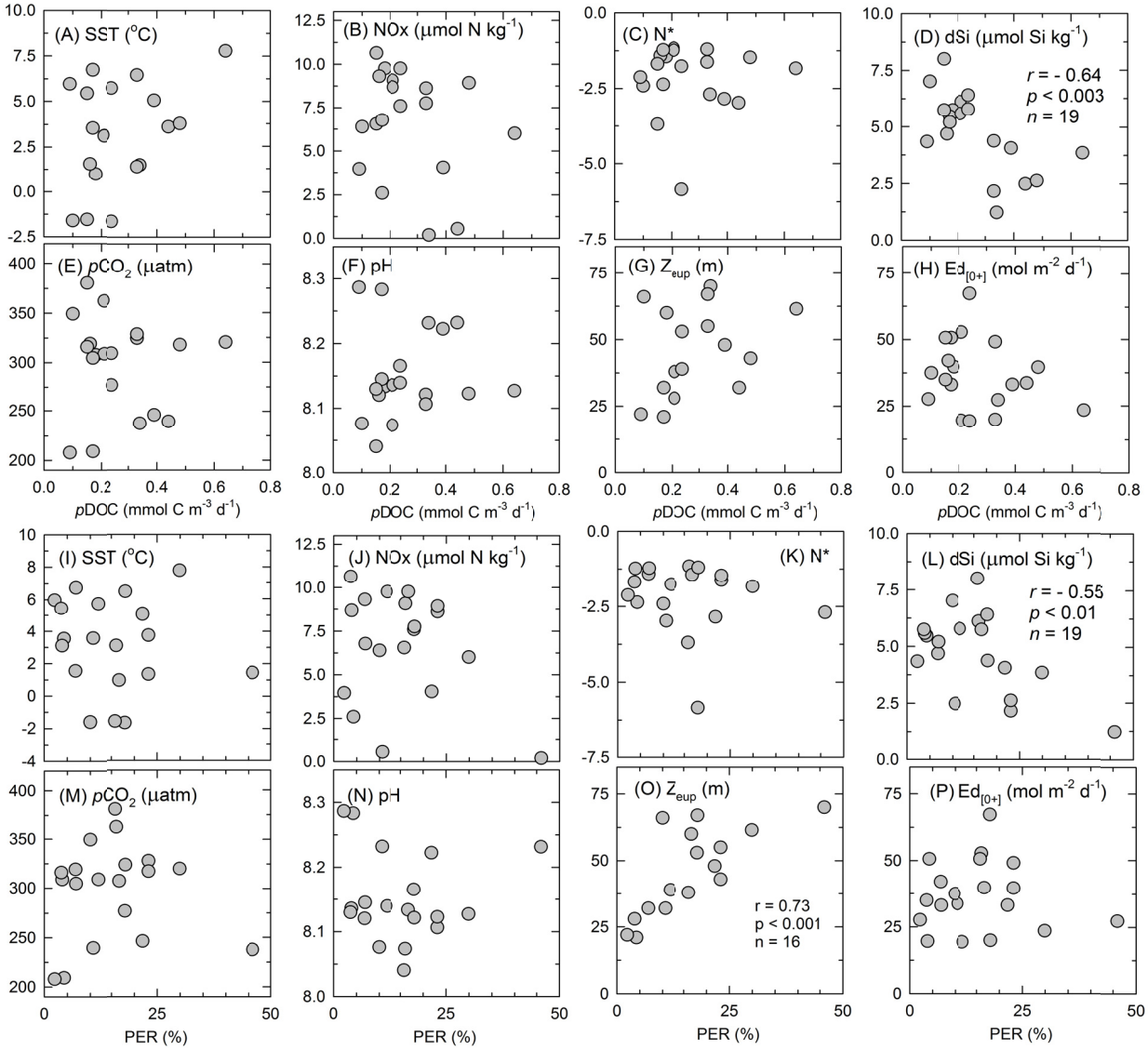
(A) SST (°C)
(B) NOx (µmol N kg-1)
(C) N*
(D) dSi (µmol Si kg-1)
r = - 0.64
p < 0.003
n = 19
(E) pCO2 (µatm)
(F) pH
(G) Zeup (m)
(H) Ed[0+] (mol m-2 d-1)
pDOC (mmol C m-3 d-1)
(I) SST (°C)
(J) NOx (µmol N kg-1)
(K) N*
(L) dSi (µmol Si kg-1)
r = - 0.55
p < 0.01
n = 19
(M) pCO2 (µatm)
(N) pH
(O) Zeup (m)
r = 0.73
p < 0.001
n = 16
(P) Ed[0+] (mol m-2 d-1)
PER (%)

Figure 4

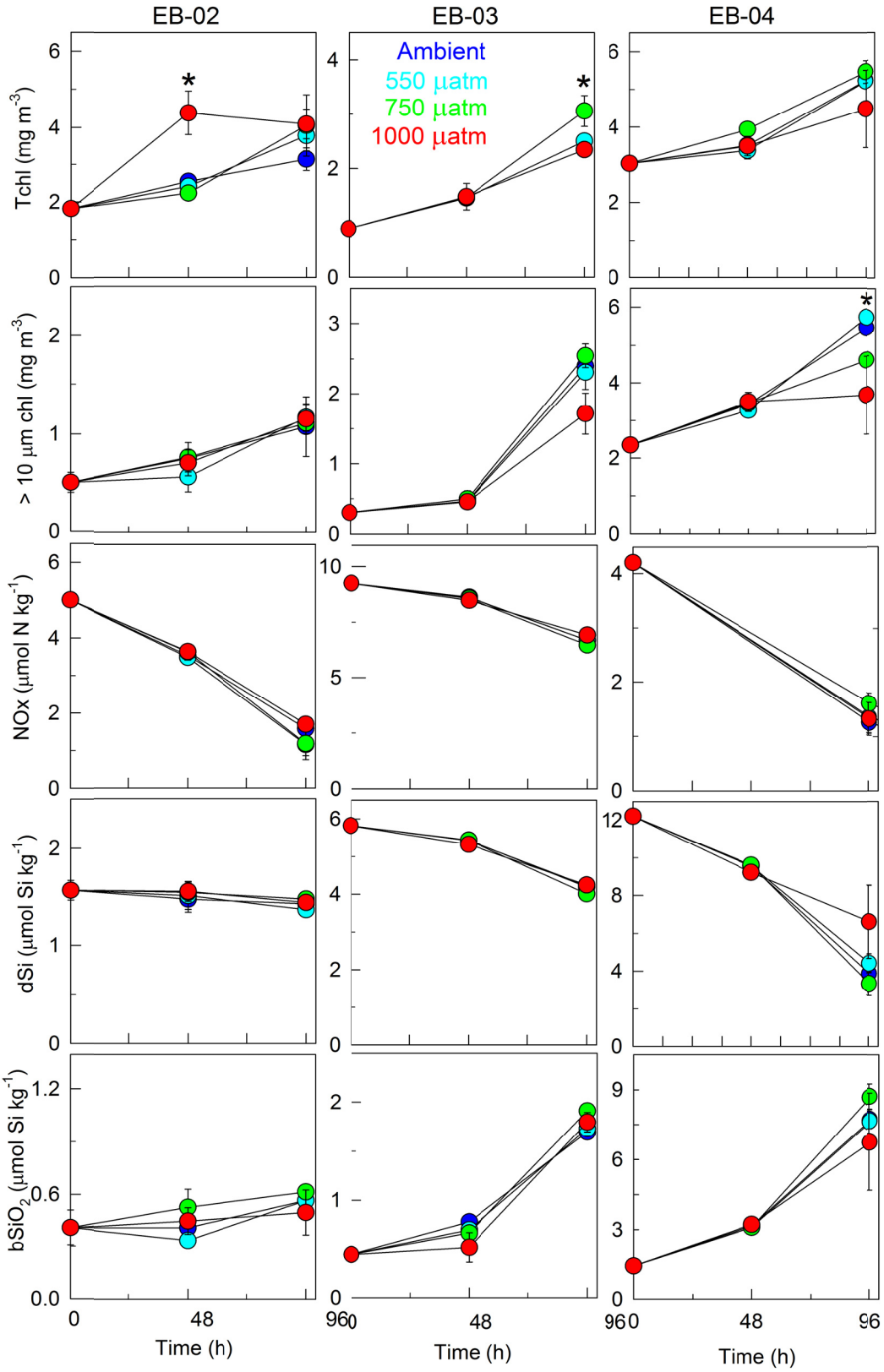
EB-02
EB-03
EB-04
Ambient
550 µatm
750 µatm
1000 µatm
Tchl (mg m-3)
> 10 µm chl (mg m-3)
NOx (µmol N kg-1)
dSi (µmol Si kg-1)
bSiO2 (µmol Si kg-1)
Time (h)
Time (h)
Time (h)

Figure 5

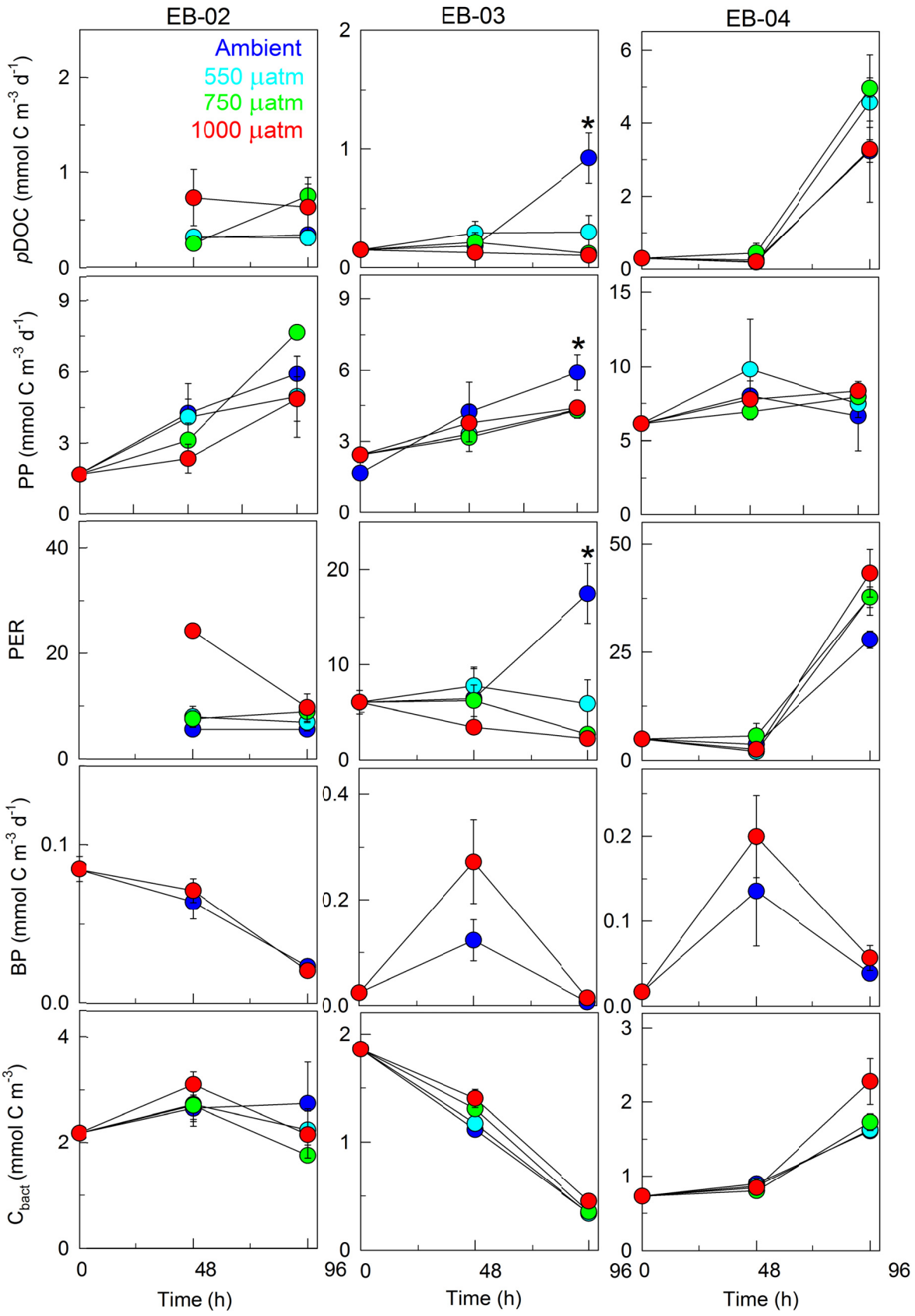
EB-02
EB-03
EB-04
Ambient
550 µatm
750 µatm
1000 µatm
pDOC (mmol C m-3 d-1)
PP (mmol C m-3 d-1)
PER
BP (mmol C m-3 d-1)
Cbact (mmol C m-3)
*
Time (h)
0
48
96

Figure 6

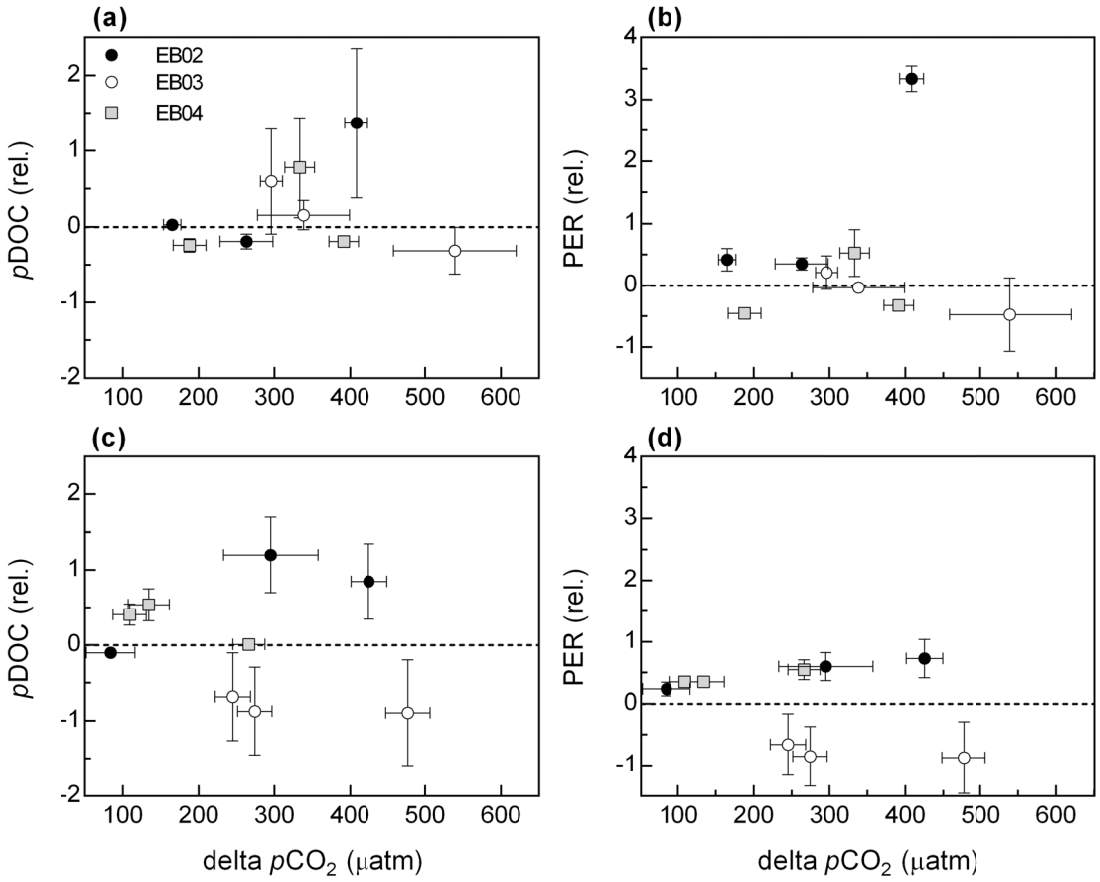
(a)
EB02
EB03
EB04
pDOC (rel.)
(b)
PER (rel.)
(c)
pDOC (rel.)
delta pCO2 (µatm)
(d)
PER (rel.)
delta pCO2 (µatm)

Figure 7

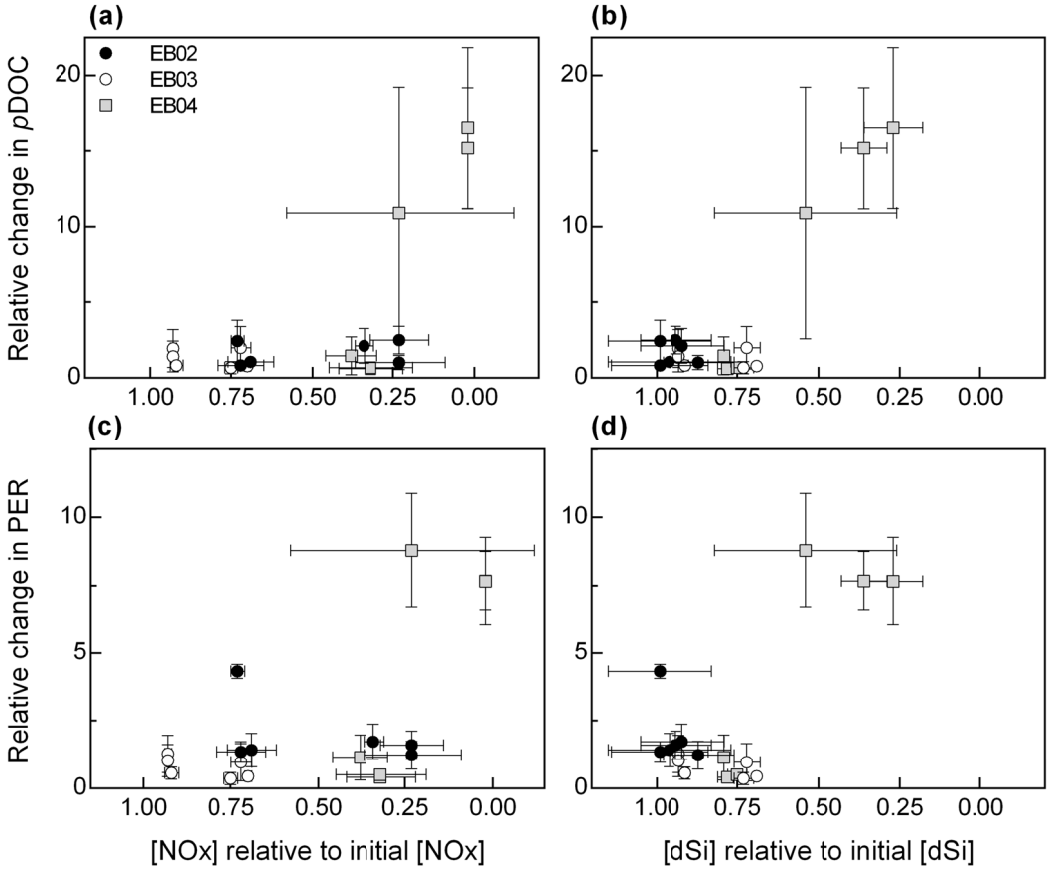
(a)
(b)
(c)
(d)
EB02
EB03
EB04
Relative change in pDOC
Relative change in PER
[NOx] relative to initial [NOx]
[dSi] relative to initial [dSi]
20
10
0
5
1.00
0.75
0.50
0.25
0.00